RESEARCH AND DEVELOPMENT REPORT
REPORT 767
28 JANUARY 1957

NEL/Report 767

AN EXPERIMENTAL MEASUREMENT OF VLF FIELD STRENGTH AS A FUNCTION OF DISTANCE, USING AN AIRCRAFT

J. E. BICKEL, J. L. HERITAGE, AND S. WEISBROD

Approved for public release;
distribution unlimited.

U. S. NAVY ELECTRONICS LABORATORY, SAN DIEGO, CALIFORNIA
A BUREAU OF SHIPS LABORATORY

The Problem

Study propagation mechanisms in the vlf and lf ranges. Specifically, determine the laws of variation of field intensity with distance, time, and location and examine the reliability of curves and formulas currently employed to predict vlf and lf field intensities.

Results

The variation of vlf field intensities with distance was recorded in an airplane to distances of 7600 km. It is found to be in closer agreement with Pierce's vlf prediction formula than any other existing formula. The observed interference pattern is satisfactorily explained on the basis of a ray model of propagation. Several graphical methods of analysis have been applied to the data and values have been obtained for reflection coefficient and phase change on reflection at the ionosphere and for the height of reflection of vlf sky waves.

Recommendations

1. Make additional recordings of vlf signal intensities by airplane, under the following conditions: (a) using improved instrumentation to obtain continuous recordings and greater accuracy; (b) recording signal to large distances to obtain propagation paths over land; and (c) continuing simultaneous recordings of multifrequency transmissions from the same general location to obtain ionospheric reflection coefficients, phase change on reflection, and height of reflection.

2. Conduct further investigations of methods for obtaining (a) actual height of reflection and phase change on reflection and (b) reflection coefficients.

3. Continue study of effects of season of the year, direction of propagation, attenuation over land vs attenuation over water, and latitude effects on variation of vlf field intensities.

Administrative Information

Work was performed under SR 06401, NE 12000-839.7 (NEL M2-1) by members of the Signal Propagation Division. This report covers work from July 1954 to December 1955 and was approved for publication 28 January 1957.

The authors wish to acknowledge the valuable assistance of H. F. Bates, J. E. Pohl, J. A. Silkwood, and flight personnel of the Fleet Airborne Electronics Training Unit, Pacific, in obtaining the flight data, and of personnel of the Naval Radio Station, 14th Naval District, for maintaining a special transmission schedule during the period in which the measurements were being made.

Contents

Illustrations

Introduction

Many early investigators have recorded vlf field intensities at fixed distances from the transmitter and used these data to establish empirical formulas for predicting vlf propagation. Primarily, the formulas represent average figures for all daytime conditions or all nighttime conditions and do not consider the variations in absorption that may occur. More recently the phase interference between modes of propagation has been taken into consideration. This interference phenomenon can be observed at a fixed distance from the transmitter by recording field intensity for varying frequencies. It can also be observed by recording field intensity as a function of distance from a transmitter where the readings are obtained so that variations of field intensity with time are minimized. An ideal method of doing this is to record field intensity in an airplane as it flies to or away from the transmitter.

Weekes[1] (see list of References at end of report) has obtained data using an airplane to 850 km from the transmitter and used the data to obtain height of reflection and reflection coefficients values. Budden[2] has applied a waveguide analysis to daytime airplane data extending to 3600 km. It is the purpose of this work to further investigate vlf field intensities out to 7000 km from the transmitter, using an airplane.

A ray theory analysis is applied to the interference pattern measured within 1000 km and values are obtained for the $||R||$ component of the ionospheric reflection coefficient, the phase change on reflection, and height of reflection of sky waves. The ray theory is also applied to the interference pattern observed for both daytime and nighttime data out to 6000 km. Comparison of the data with existing vlf field intensity formulas is made.

Instrumentation

To measure vlf signals, a Navy P2V patrol plane was equipped with a URM-6 receiver. The 12-kc i-f output of the receiver was displayed as an oscilloscope presentation from which the peak deflection of Morse-keyed signals could be visually obtained and recorded by an observer in the aircraft. The gain of the receiver-oscilloscope combination was frequently recalibrated from a known voltage injected into the receiver input through a dummy antenna.

The vlf receiving antenna was a vertical whip mounted near the intersection of wing and fuselage. Preliminary experimental tests were made to make certain that this antenna had no appreciable response to fields of polarization other than vertical. In level flight, signal reading was independent of aircraft heading in both the near and far vlf fields. The measured signal strength decreased considerably when the aircraft was banked. Flight paths on radial courses from the vlf transmitter in the region dominated by the groundwave and one-hop skywave had amplitude maxima and minima occurring at identical ranges for altitudes of 1000 and 10,000 feet. From these tests it was inferred that the measuring system in the aircraft was responding only to the vertical component of electric field under conditions of level flight.

To convert the relative field strength obtained in the aircraft to absolute field strength, the system was calibrated in flight. The aircraft was flown at a low altitude over a ground monitor with known calibration or was flown for some distance in the field of a transmitter of known radiated power where the field intensity is varying inversely as the distance from the transmitter. However, when the data are normalized to one kilowatt of radiated power it is not necessary to use either the calibration factor for the recording system or the radiated power in calculation if the relative received voltage is recorded in the near field of the transmitter where it varies inversely with distance. The data are plotted so that on inverse distance field strength of 69.5 db above one microvolt per meter corresponds to a distance of 100 km.

Sources of Data

The data reported here were obtained on three different expeditions. The first, during September 1954, was a "circle" trip from San Diego to San Francisco, Hawaii, Wake Island, Tokyo, Adak, Kodiak, Seattle, to San Diego. The principal station recorded was NLK near Seattle, Washington, transmitting on 18.6 kc. Flight schedules were arranged so that the maximum amount of data from NLK could be obtained while the transmission path was sunlit. Other stations recorded on this flight include NSS near Washington, D. C. (19.0 kc), NPM at Hawaii (16.6 kc), and NDT near Tokyo (17.4 kc).

The second trip, in December 1954, was from San Diego to Hawaii and return, the outgoing leg

being flown in the daytime and the incoming leg at night. During this trip four transmissions were recorded simultaneously. They were 16.6-, 19.8-, and 40-kc transmissions from Hawaii, and a 30-kc signal from San Diego.

The third flight was a round trip from San Diego to Tokyo, the return via Hawaii and Wake Island. The outgoing flights were made at night and the return flights in daytime. The 16.6-kc signal from Hawaii was recorded throughout the trip. On some of the incoming daytime flights the 40-kc transmission from the same location was recorded simultaneously with the 16.6-kc data.

The accuracy of the data is limited by uncertainties in the values of radiated power, received signal amplitude, and aircraft position.

The error due to the combined effect of errors in aircraft position and received signal amplitude, for measurements in the inverse distance field where the effect of aircraft position on signal intensity is most pronounced, is estimated to be about ± 1.0 db, with extreme variation of ± 1.5 db. This estimate of error was determined from data taken from NPM on 16.6 kc during transmissions when variations in transmitter radiated power were accurately monitored. The variation in radiated power level is of the order of ± 1.0 db. The error in received signal amplitude is of the order of ± 0.5 db for most of the data out to about 4000 km and is about ± 1.0 db or more at larger distances where signal-to-noise ratio was poor. Near the middle of long over-water flights the aircraft position was known to about ± 10 miles. This positional error is insignificant beyond about 500 km from the transmitter in the type of analysis used in this report. Therefore the total estimated error of the data, in the region where positional error is insignificant, is about ± 1.5 db or ± 2 db.

This measurement error affects the accuracy with which the values of reflection coefficient $||R||$ and apparent height of reflection h' can be determined from the data. The accuracy of calculated $||R||$ and h' values are also limited by the insufficient number of measurements made for a given distance, especially within 1000 km of the transmitter. This type of limitation will be discussed below in the section concerned with the method of analysis. (See refs. 7 and 9 for definition of symbols.)

Comparison of Daytime Data with Theoretical Transmission Formula

Figure 1 is a composite presentation of all daytime data obtained from NPM on 16.6 kc, normalized to one kilowatt of radiated power. A smooth curve has been drawn through the measured points. The straight line represents the theoretical inverse-distance dependence of field intensity. The flights were planned so that the maximum amount of data was obtained while the transmission path was sunlit. However, on the longest of the three flights (the Hawaii to San Diego path), the data also include measurements at the beginning and end of the flight, recorded during the times of transition from day to night.

Inspection of figure 1 shows that in general the data recorded on the various flights are consistent within 4 db at any range. There are three major exceptions. The first, in the region of 500-600 km, is presumably due to interference between the ground wave and the one-hop skywave. The total field intensity is subject to wide variations corresponding to relatively small variations in ionospheric height and ionospheric reflection coefficient. This type of dip will be considered in greater detail in the following section.

The second exception is for the flight of December 1954 in the 2700-to-3600-km region. The lower field strength recorded in this instance may be an example of increased ionospheric absorption of vlf radio waves.

The high signal intensity recorded in September 1954 for the 4650-to-6200-km region is uncertain and may have been caused by equipment malfunction.

Figure 2 is a composite plot of the daytime data obtained from the stations other than the 16.6-kc transmission from Hawaii. The same general behavior of field strength with distance as indicated in figure 1 occurs here with one major exception. The recording of NLK (Seattle) field strength on the flight from Tokyo to Seattle via Adak and Kodiak is consistently lower than the other recorded data. These data are for the northernmost propagation path. The reduction in signal intensity may indicate a tendency for higher absorption to occur in the higher latitudes. The data obtained from NSS (Washington, D. C.) in the 4500-to-7200-km region are for a propagation path which

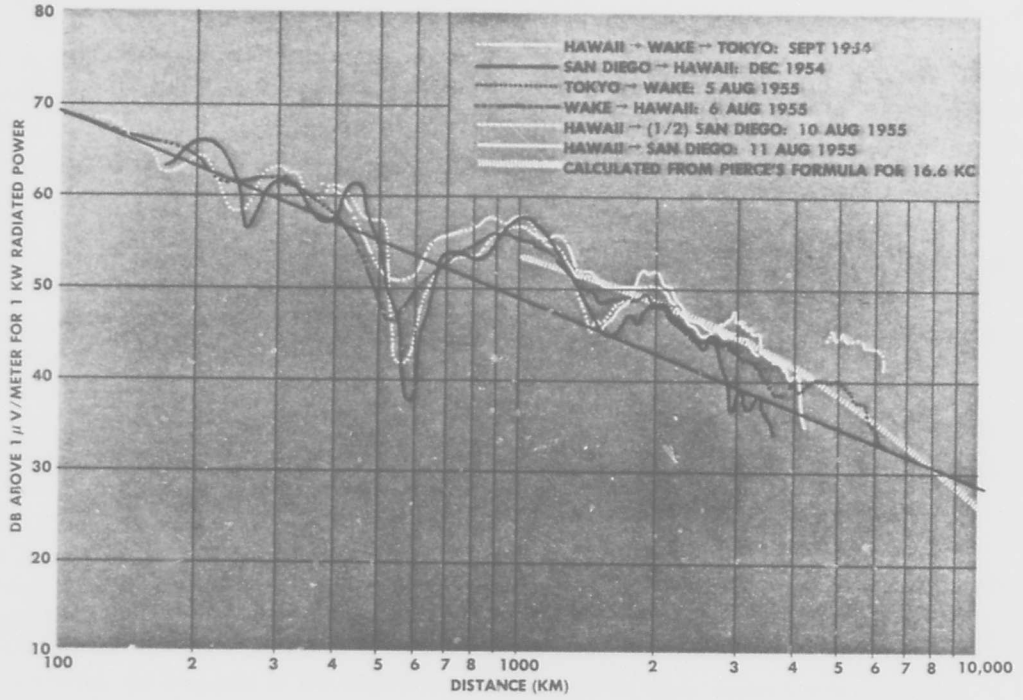

Figure 1. All daytime data from NPM on 16.6 kc, compared with calculations from Pierce's formula.

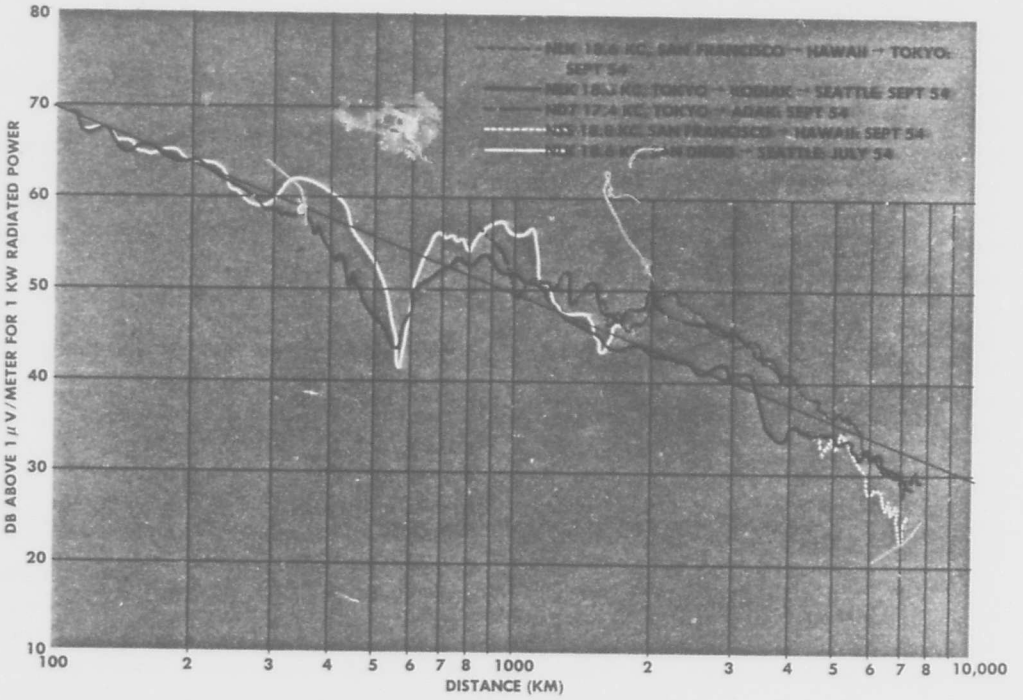

Figure 2. All daytime data from NLK, NDT, and NSS.

passes over the continental United States. The apparent additional attenuation due to propagation over 3800 km of land instead of water seems to be about 3 db for this case. However, there is some uncertainty in the aircraft calibration for this data.

The older empirical formulas that have been used to predict daytime vlf field intensity E are:

$$\text{Austin-Cohen } E \propto \frac{1}{d}\left(\frac{\theta}{\sin\theta}\right)^{1/2} \exp\left[-(0.001d/\lambda 0.6)\right]$$

$$\text{Espenschied-Bailey } E \propto \frac{1}{d} \exp\left[-(0.005d/\lambda 1.25)\right]$$

$$\text{Baldwin-McDowell } E \propto \frac{1}{D} \exp\left(-0.000013fD\right)$$

where

d = distance from transmitter (km)

D = distance from transmitter (nautical miles)

θ = subtended range angle at the earth's center (radians)

λ = wavelength (km)

f = frequency (kilocycles per second)

Kitchen, Pressey, and Tremellen[3] show that the Baldwin-McDowell formula predicts a higher field intensity at all distances out to 12,000 km at 18 kc. All formulas give a predicted field intensity which is everywhere below the inverse-distance field. The Baldwin-McDowell and Espenschied-Bailey formulas use the inverse-distance field multiplied by an empirical exponential attenuation factor. The signal calculated from the Austin-Cohen formula, in the case where absorption is absent, exceeds the inverse distance field by $\sqrt{\theta/\sin\theta}$. This factor is negligible for short distances and is about 2 db at 6000 km. For a formula to represent accurately the daytime field intensities recorded out to about 6000 km, it must indicate field intensities greater than the inverse-distance field. The inverse-distance relationship describes only the field of an antenna over a perfectly conducting earth when no energy is reflected by an elevated layer.

However, the distant vlf field is primarily the resultant of energy contributions propagated via skywave modes. Pierce,[4] by summing up the unabsorbed intensities of individual skywaves, calculates that the rms value of the distant field (neglecting the relative phases of the component skywaves) should be 4.5 db above the inverse-distance value at 1000 km, with the difference increasing with distance. Pierce's formula is:

$$E = 2000\mu v/m\left(\frac{P\cos^4\alpha}{h\sin\theta}\right)^{1/2} \exp\left(-k\theta\right)$$

where

P = radiated power in kilowatts

α = angle from the ground plane at which skywaves radiate from the antenna

θ = subtended range angle at the earth's center (radians)

h = height of reflecting layer

k = attenuation factor

The attenuation factor k is a function of the solar zenith angle, the type of terrain over which the signal propagates, and the frequency.

An approximate relation which is useful beyond 1000 km is obtained by assuming that $\cos\alpha = 1$ and $h = 75$ km for daytime propagation. The equation then reduces to

$$E = 231\mu v/m\left(\frac{P}{\sin\theta}\right)^{1/2} \exp\left[-(0.1f)^u\theta\right]$$

where

f = frequency of signal in kilocycles per second

$$u = \begin{cases} 0.5 \text{ for transmission over sea water at night} \\ 0.65 \text{ for transmission over land at night} \\ 0.9 \text{ for transmission over sea water by day} \\ 1.05 \text{ for transmission over land by day} \end{cases}$$

This approximate equation was used to calculate the field intensity out to 10,000 km. The results of this calculation for 16.6 kc are shown plotted in figure 1 and for 18.6 kc in figure 3 where $u = 0.9$. The results of calculations using the Baldwin-McDowell formula for 18.6 kc are also shown in figure 3, with the data recorded at 18.6 kc. Since the Baldwin-McDowell formula predicts a higher field intensity at all distances than the Espenschied-Bailey or Austin-Cohen formulas, it may be inferred from figures 1 and 3 that Pierce's formula gives the most accurate representation of the daytime field intensities which were recorded.

Ray Model Concepts Used in the Analysis of the Data

A simple ray model of vlf propagation was assumed in an attempt to fit the experimental data. Figure 4 illustrates this model which assumes that the field intensity at any distance from the transmitter is equal to the vector sum of components resulting from the ground wave, one-hop, two-hop, and whatever other sky waves may be significant. The amplitude of the ground wave is obtained from calculations of K. A. Norton.[5]

The amplitude of each sky wave can be considered as the unabsorbed sky wave amplitude multiplied by a factor that is a function of the reflecting properties of the ionosphere. Figure 5 shows the results of calculation of the unabsorbed one-hop sky wave amplitude at varying distances as would be observed in an aircraft flying at 10,000 feet altitude. The straight line represents the inverse-distance relationship for one kilowatt of radiated power. The dashed line is the amplitude that would be received on the surface of the earth from a short vertical radiator with a cosine pattern if the focusing effects of a spherical ionosphere were neglected. The solid lines represent the unabsorbed signal intensity where the focusing factor, as calculated by Pierce,[4] is included in the calculations. The focusing factor is negligible within about 1000 km but is very significant near the limiting distance for one-hop sky wave where it theoretically becomes infinite. The variation in amplitude shown for distance less than 1000 km for the different frequencies results from destructive interference between the ground-reflected sky wave and the direct sky wave received in an aircraft flying at 10,000 feet altitude.

The effect of "antenna cutback" on the distant sky wave field intensity, for the case where the antenna is surrounded by sea water, is shown by the dotted curve of figure 5. "Antenna cutback" is defined here as the reduction in the intensity of radiation from vlf antennas at low angles. The total sky wave intensity is considered here to be represented by the vector sum of radiation from the antenna itself and its image. Therefore, the reflecting properties of the earth in the immediate vicinity of the antenna affect the shape and magnitude of the cutback of the antenna pattern. Calculations for the curve of figure 5 are based on the reflection coefficients of sea water at 15 kc as given by Terman.[6] The effect of "antenna cutback" on the vertical radiation pattern of an antenna is given by Pierce[4] for varying distances.

The attenuation factor by which the unabsorbed one-hop sky-wave amplitude must be multiplied to obtain its actual value is the $||R||$ component of the ionospheric reflection coefficient, since both transmitting and receiving antennas were designed for vertical polarization. For the *n*-hop sky wave the attenuation factor would be represented by the vector combination of $||R||^n$ with terms involving the product of $||R|_{\perp}$, $|_{\perp}R||$, and $|_{\perp}R|_{\perp}$, assuming the ground-reflection coefficient is unity. For the large distances and oblique angles involved where multi-hop rays are significant, Budden[7] has shown that the conversion coefficients $|_{\perp}R||$ and $||R|_{\perp}$ are small compared to the $||R||$ factor. Therefore, only the $||R||^n$ term was used as the attenuation factor for the *n*-hop sky wave with the ground-reflection coefficient assumed to be unity.

Consideration has been given to the possibility that the sharp cutoff of the sky wave at limiting distance due to the earth's curvature does not really exist, but instead that the sky wave energy continues to propagate as a ground wave beyond the earth's curvature. This consideration has been incorporated in the analysis of data from one flight from which the amplitude of individual sky waves as a function of distance were estimated. The calculated vector sum obtained agrees well with the measured field intensities.

The relative phases of the contributing rays were also calculated on the basis of the simple ray model. For a given frequency, the height at which sky waves are reflected, the changes of phase of the wave fronts upon reflection, the distance from the transmitter, and the velocity of propagation of the ground wave with respect to the sky waves all affect the relative phase of the rays. The effect of ionospheric height on the phases of the vectors were calculated using the geometrical path-length differences between the various modes of propagation. The set of curves in the lower left-hand corner of figure 6 is one type of graphical presentation used to represent the relation between height of reflection, distance from the transmitter, and phase relation between vectors representing two modes of propagation. These curves represent the ground wave and one-hop sky wave. The solid lines represent loci of points for which the relative phase is constant as

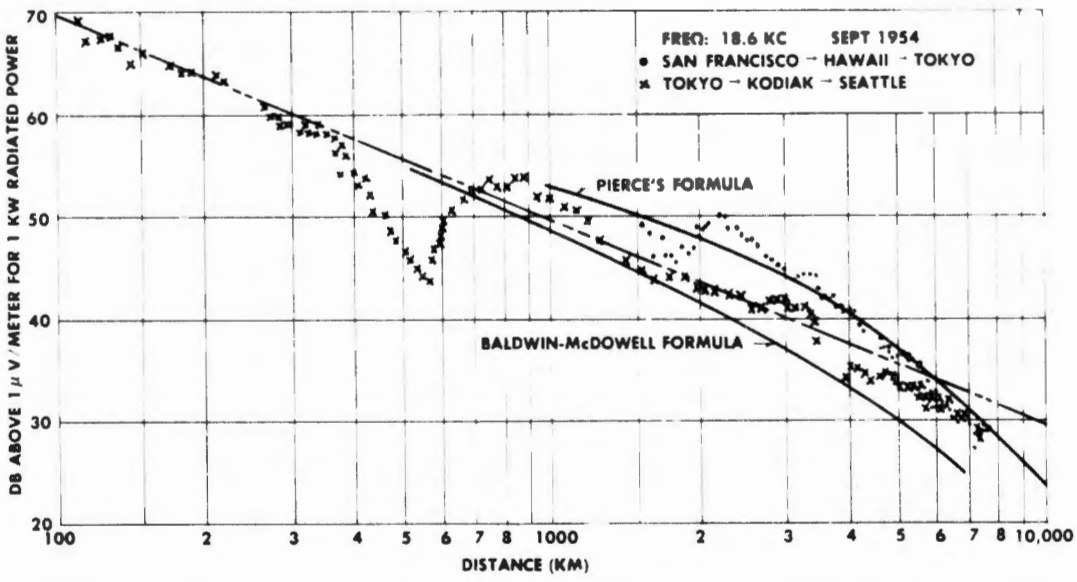

Figure 3. Daytime data from NLK recorded at 18.6 kc compared with calculations based on Pierce's formula and the Baldwin-McDowell formula.

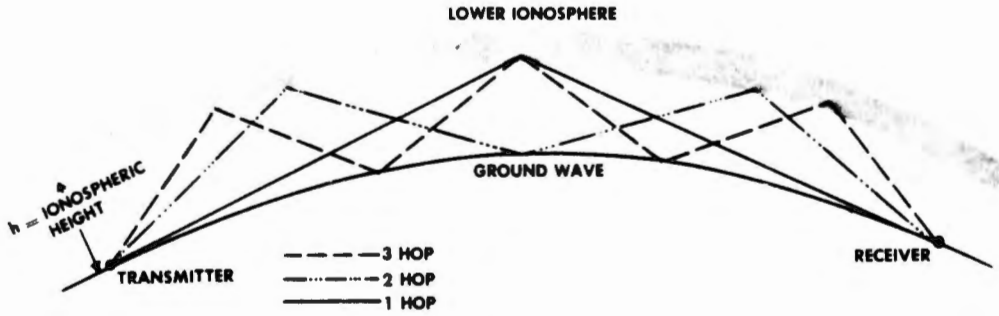

Figure 4. Ray model of vlf propagation.

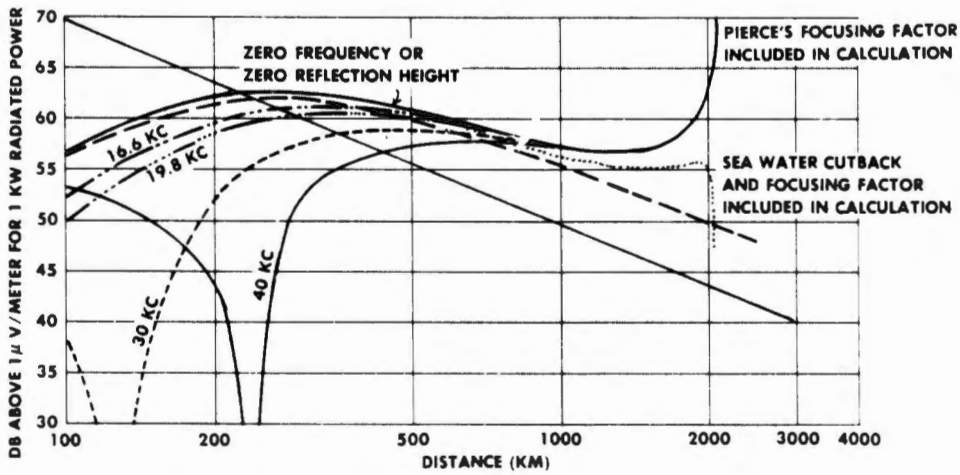

Figure 5. Calculation of vertically polarized, unabsorbed, one-hop sky-wave amplitude, reflected from height of 90 km, as seen from 10,000 ft altitude.

reflection height and distance are varied, assuming that the ground wave and sky wave both propagate with free-space velocity. Each curve corresponds to a particular value of constant path-length difference between the two modes of propagation. If there is no phase change on reflection from the ionosphere, the vectors will be in phase for integral number of wavelengths and out of phase for integral number of half-wavelengths. The dashed lines in figures 11-13 are for the case where the ground-wave velocity is 0.14 per cent less than the sky-wave velocity, as indicated by Mendoza.[8] For greater distances where higher-order hops are of greatest importance, phase interference curves between successive higher order hops were calculated.

The apparent height of reflection h' is determined from the position of the maxima and minima in the data using phase relationship curves similar to figure 6, assuming no phase shift on reflection. This method was used successfully for distances less than 1000 km where only the ground wave and one-hop sky wave need be considered. At greater distances, it is difficult to determine which modes of propogation are predominant because of the uncertainty in sky wave amplitudes. There are also regions where three vectors must be considered to obtain the resulting amplitude.

In the near region where ground-wave and one-hop sky wave predominate, the amplitude of the one-hop sky wave can be determined from the magnitude of the variation of measured field from the ground-wave amplitude. The ratio of the sky-wave amplitude to the calculated unabsorbed sky-wave amplitude gives an estimate of the reflection coefficient $||R||$.

Results of Ray Theory Analysis of Daytime Data

The daytime data that have been analyzed for apparent height of reflection and reflection coefficient are plotted in figures 6-13. Each of these figures shows the approximate time from sunrise or sunset that the plane was over the transmitter. Approximately 3 hours were required to fly 1000 km. Each figure also gives the direction from the transmitter for which the data were taken and indicates whether the airplane was flying toward or away from the transmitter. Both the 16.6-kc and 40-kc transmitters are located in the Hawaiian Islands at 158° W longitude and 21.5° N latitude.

The corresponding apparent height of reflection is shown in the lower left section of each figure. In determining the height curves of figures 6-10 it was assumed the ground wave travels with free space velocity and that no phase change occurs upon reflection from the ionosphere. The same assumptions were made for the determination of the height curves labeled A_1 in figures 11-13.

From comparison of the height curves of the 16.6-kc data two types of results are indicated. The data of figures 7, 9, 10, and 11 give height values which tend to increase regularly with distance and everywhere are within 3 km of each other. The data of figures 6 and 8 show a partial minimum at 360-km distance indicating a sudden increase in the apparent height of reflection at that distance. This effect could be produced by a fast change in ionospheric reflection conditions either as a function of time or angle of incidence. These data also indicate that at 200 km h' is about 3 km greater than it is for the first group of data. No consistent diurnal or seasonal height variation is evident from the 16.6-kc daytime data.

In figures 11-13, the height curves labeled A_2 are obtained with the assumptions that the ground wave travels with a velocity which is 0.14 per cent less than free-space velocity and that no phase change occurs on reflection from the ionosphere. The height curves labeled B are obtained with the assumption of a 180° phase advance on reflection from the ionosphere. The curves labeled B_1 correspond to a ground-wave velocity equal to that of free space and those labeled B_2 were obtained using the reduced ground-wave velocity. The two sets of height curves of figures 12 and 13 for the 40-kc data illustrate that there is no single height which satisfies the data of any frequency. The height curves shown with the 16.6-kc data are considered to be the most probable, as the reflection heights obtained are consistent with height of reflection values reported by other investigators in ionospheric research.

Figures 14A and 14B show the height curves from the simultaneously recorded 16.6-kc and 40-kc data of 6-7 August. If the assumption is made that both 16.6-kc and 40-kc sky waves are reflected from the same actual height, and that the phase change upon reflection for both frequencies is the same, it is possible to determine these two parameters. The dotted height curve of figures 14A and 14B is the height of reflection obtained in this way. The asso-

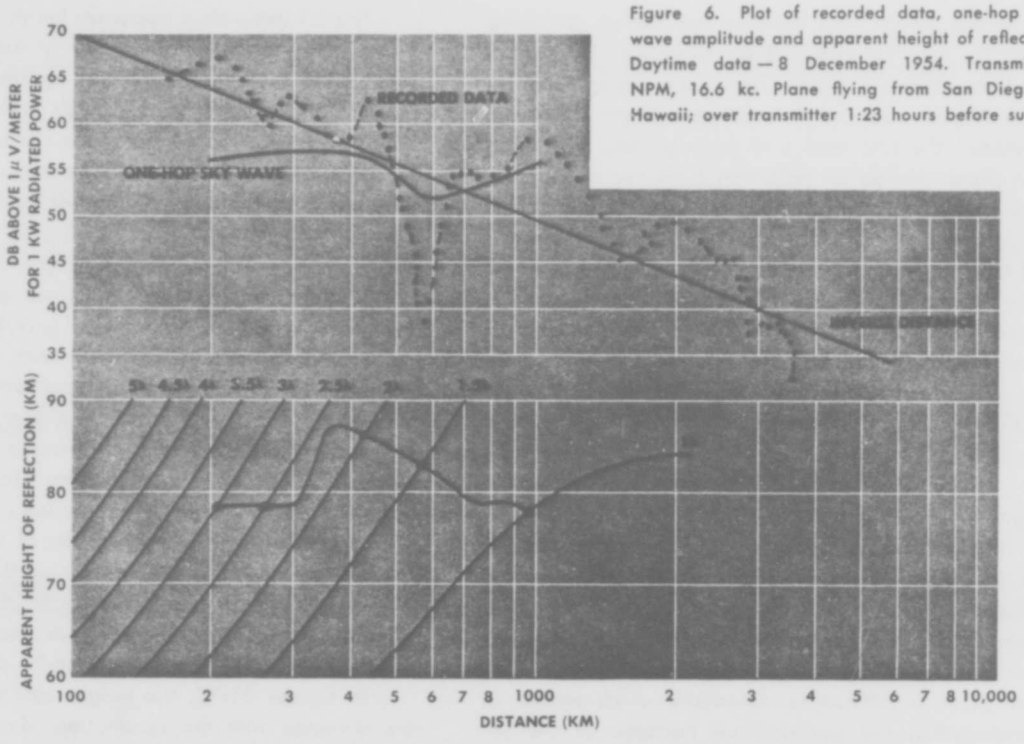

Figure 6. Plot of recorded data, one-hop sky-wave amplitude and apparent height of reflection. Daytime data — 8 December 1954. Transmitter: NPM, 16.6 kc. Plane flying from San Diego to Hawaii; over transmitter 1:23 hours before sunset.

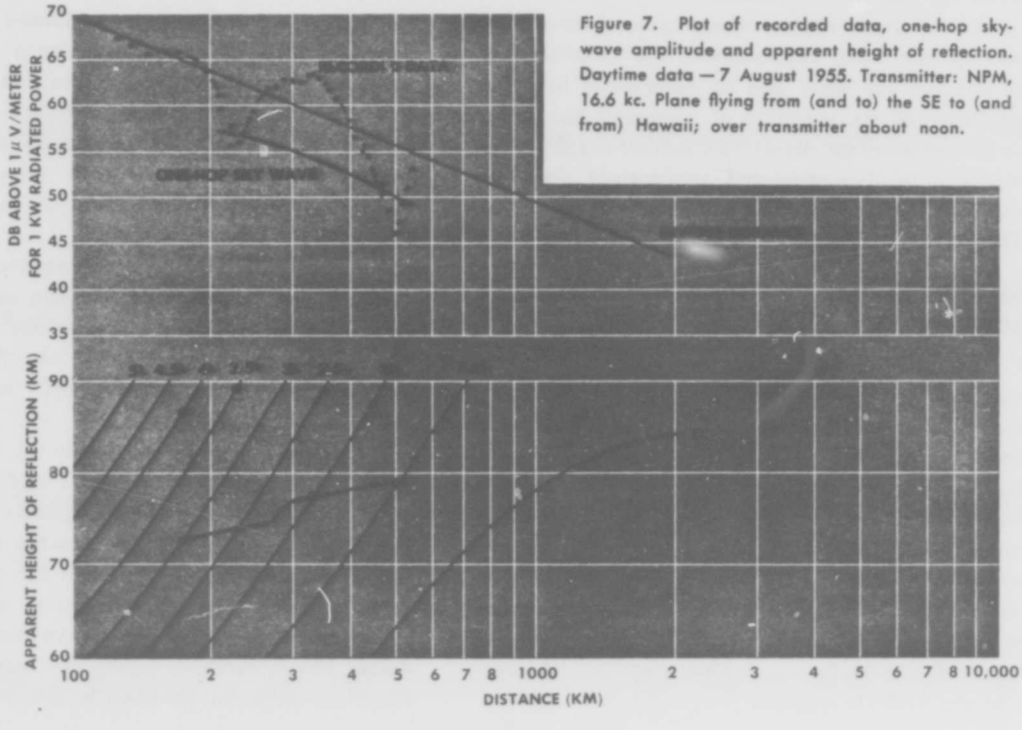

Figure 7. Plot of recorded data, one-hop sky-wave amplitude and apparent height of reflection. Daytime data — 7 August 1955. Transmitter: NPM, 16.6 kc. Plane flying from (and to) the SE to (and from) Hawaii; over transmitter about noon.

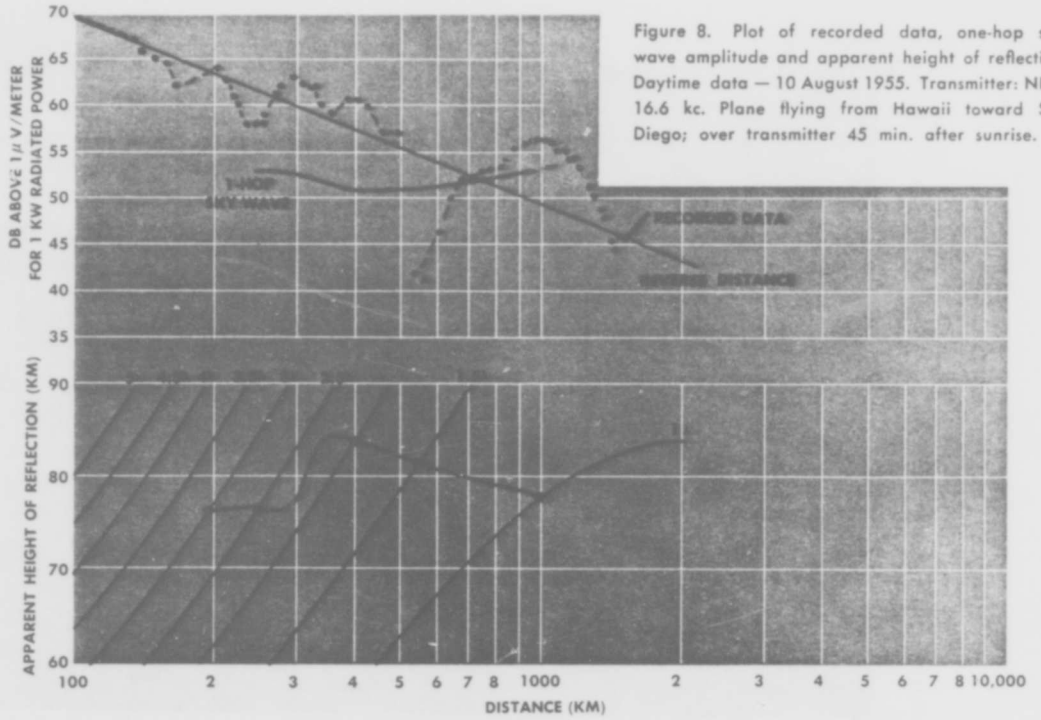

Figure 8. Plot of recorded data, one-hop sky-wave amplitude and apparent height of reflection. Daytime data — 10 August 1955. Transmitter: NPM, 16.6 kc. Plane flying from Hawaii toward San Diego; over transmitter 45 min. after sunrise.

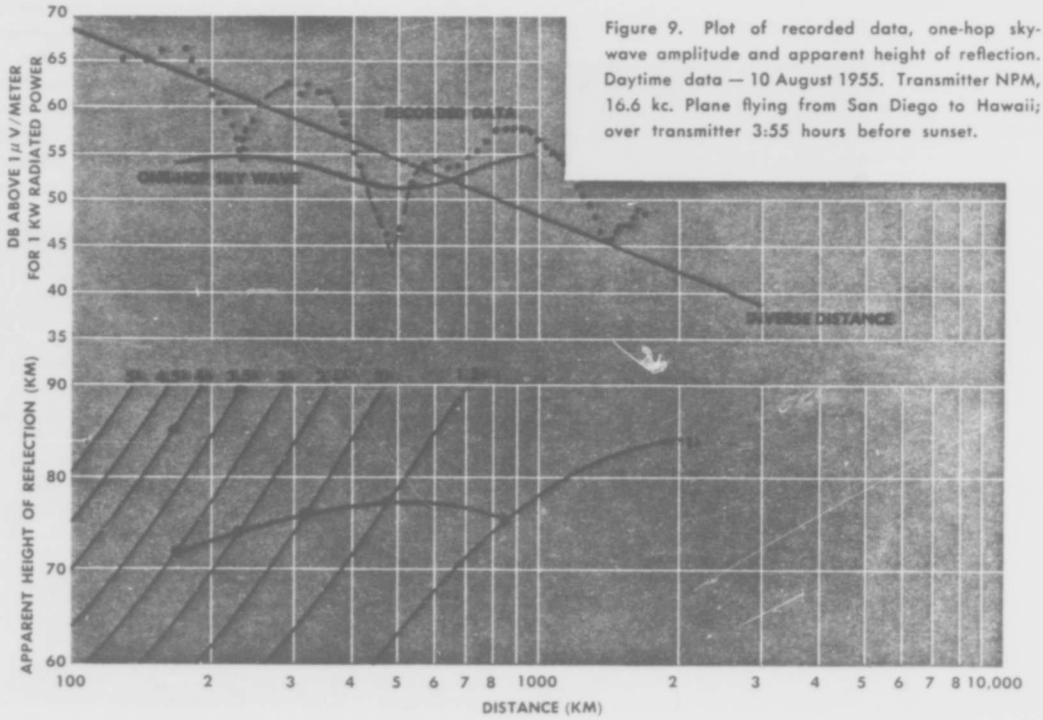

Figure 9. Plot of recorded data, one-hop sky-wave amplitude and apparent height of reflection. Daytime data — 10 August 1955. Transmitter NPM, 16.6 kc. Plane flying from San Diego to Hawaii; over transmitter 3:55 hours before sunset.

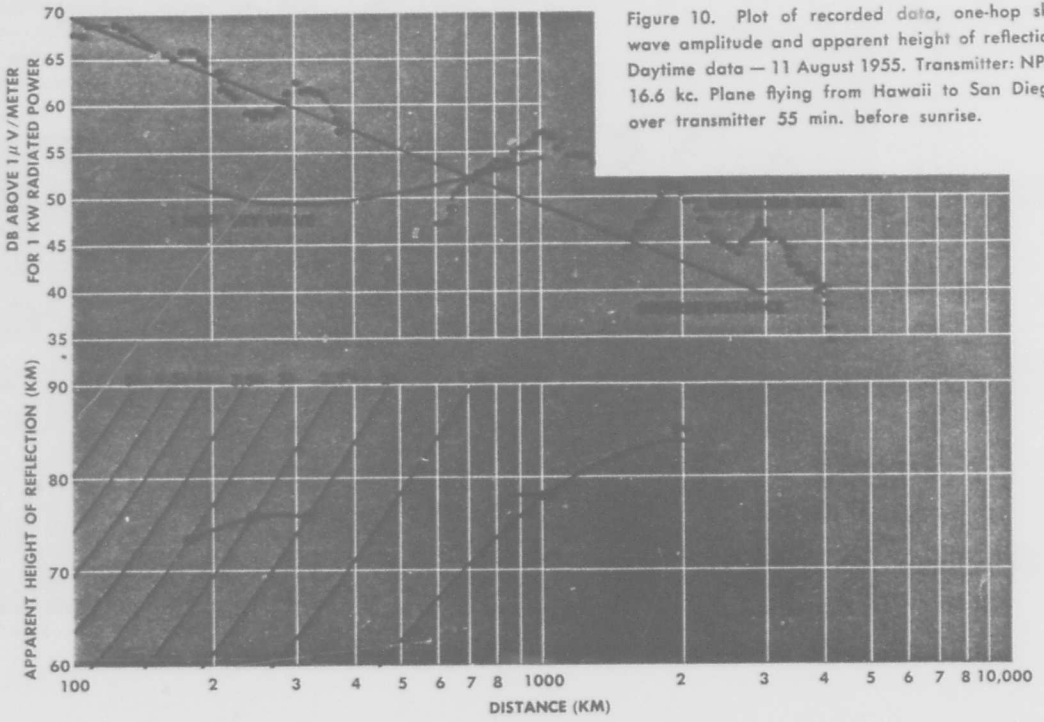

Figure 10. Plot of recorded data, one-hop sky-wave amplitude and apparent height of reflection. Daytime data — 11 August 1955. Transmitter: NPM, 16.6 kc. Plane flying from Hawaii to San Diego; over transmitter 55 min. before sunrise.

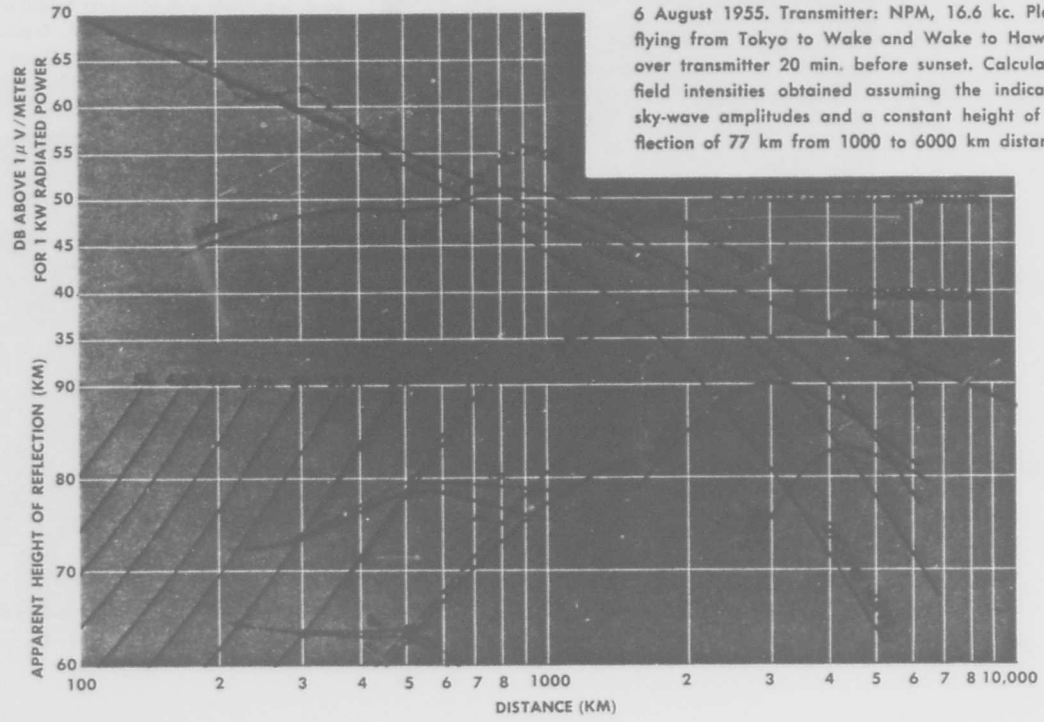

Figure 11. Plot of recorded data, ground-wave amplitude, assumed sky-wave amplitudes, and apparent height of reflection. Daytime data — 5 and 6 August 1955. Transmitter: NPM, 16.6 kc. Plane flying from Tokyo to Wake and Wake to Hawaii; over transmitter 20 min. before sunset. Calculated field intensities obtained assuming the indicated sky-wave amplitudes and a constant height of reflection of 77 km from 1000 to 6000 km distance.

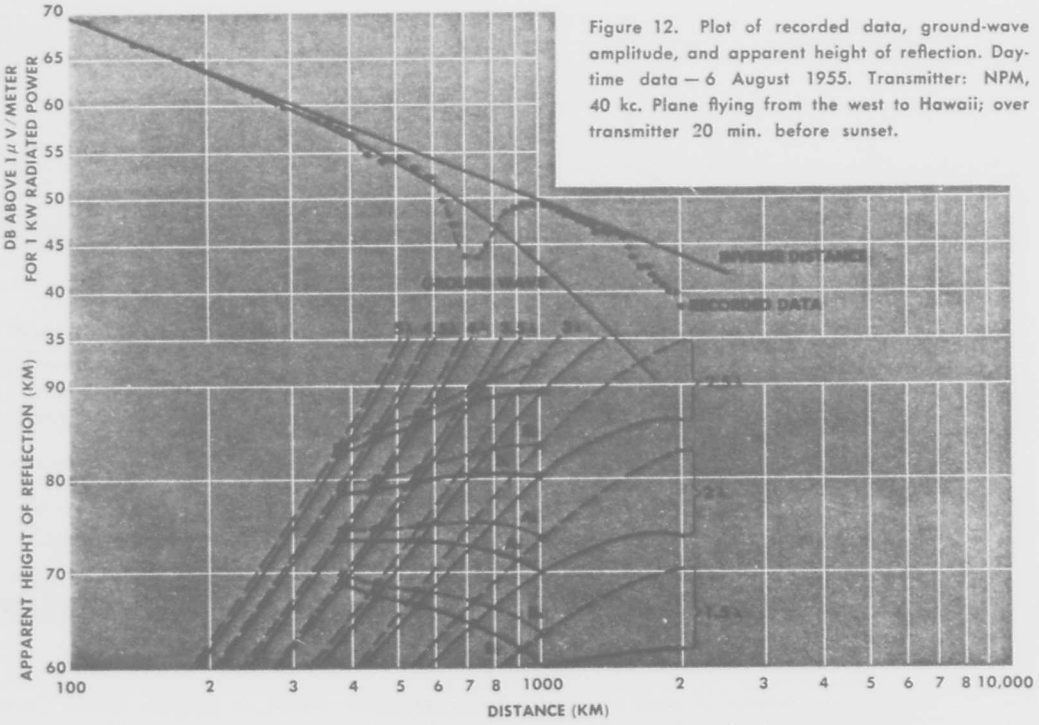

Figure 12. Plot of recorded data, ground-wave amplitude, and apparent height of reflection. Daytime data — 6 August 1955. Transmitter: NPM, 40 kc. Plane flying from the west to Hawaii; over transmitter 20 min. before sunset.

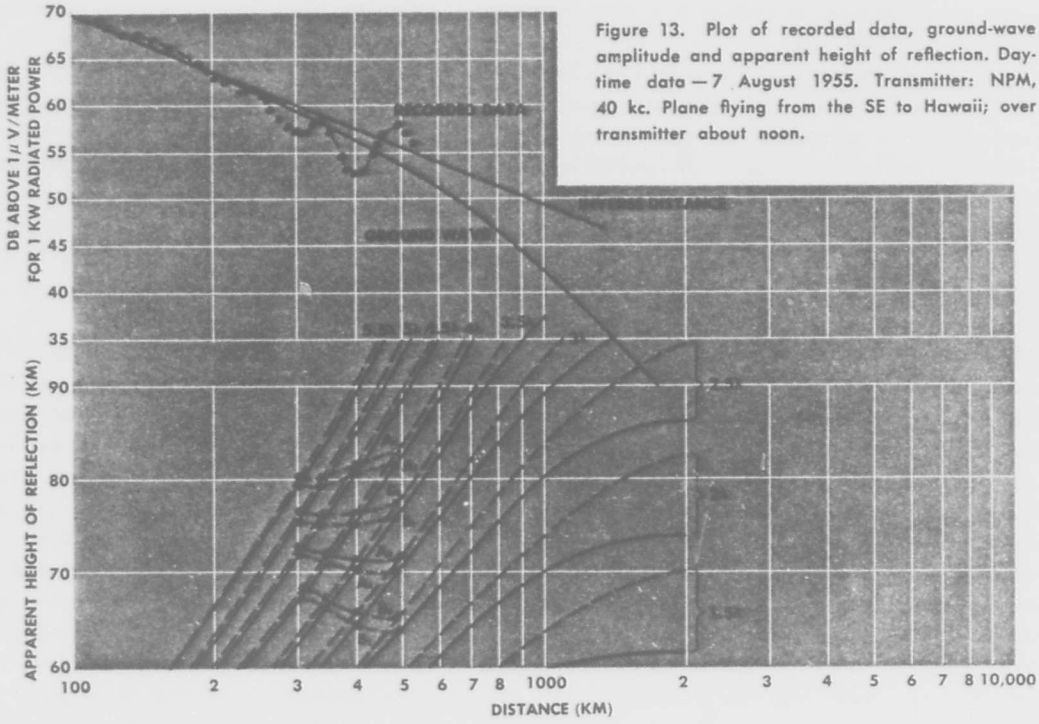

Figure 13. Plot of recorded data, ground-wave amplitude and apparent height of reflection. Daytime data — 7 August 1955. Transmitter: NPM, 40 kc. Plane flying from the SE to Hawaii; over transmitter about noon.

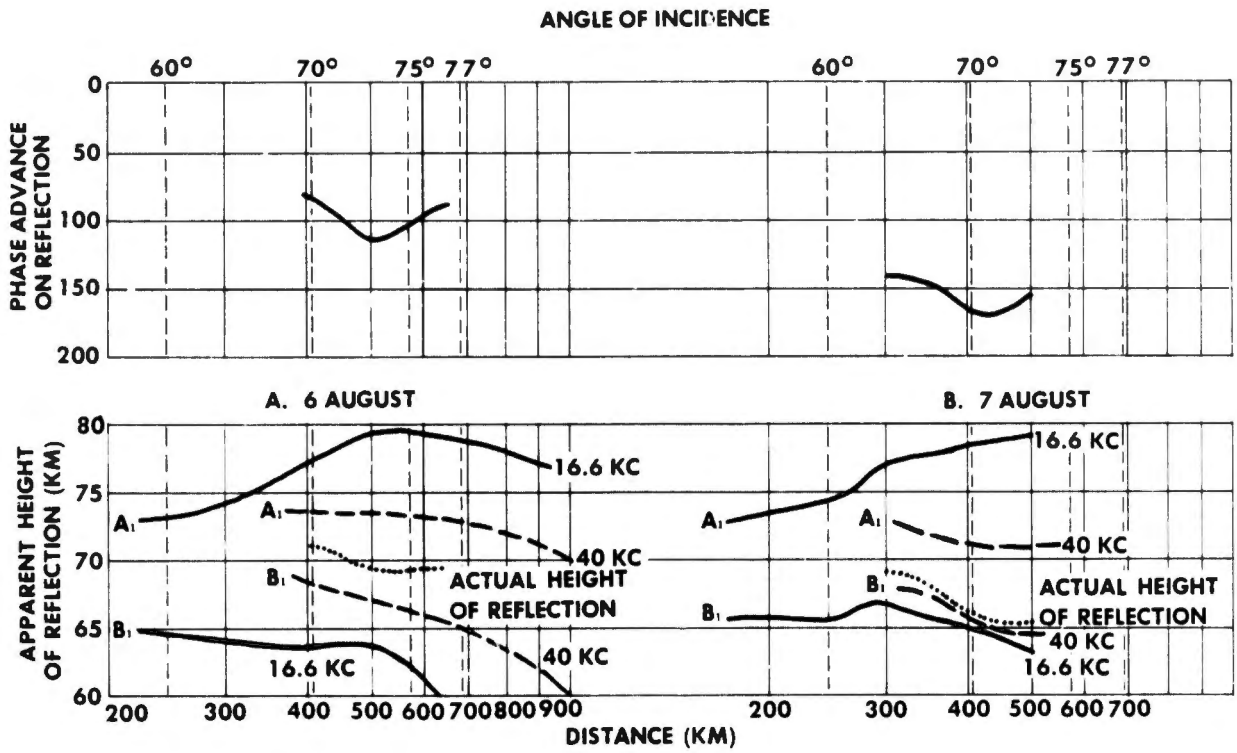

Figure 14. Calculation of actual height of reflection and phase change on reflection from two simultaneously recorded frequencies.

ciated phase change on reflection is also indicated in figures 14A and 14B.

Wait and Perry[9] give theoretical results of vlf reflection coefficient as a function of frequency. Inspection of their calculated curves of phase change upon reflection indicates that in general it does vary with frequency. However, the variation is small for ionospheric conditions which may be assumed to exist during a summer day. Therefore, the assumption of equal phase change on reflection for 16.6 kc and 40 kc appears reasonable.

A second method of analysis has been used to obtain the actual height of reflection and the phase change on reflection. It is based on the assumption that these two parameters are relatively constant between successive maxima and minima of the data. This method of analysis is also a graphical one in which is used a family of curves showing height of reflection as a function of path-length difference between ground wave and one-hop sky wave for a set of ground distances. These curves are shown in figure 15. The path-length difference along the ordinate is shown both in kilometers and in half-wavelength increments for 16.6 kc, which is further divided into degrees representing a phase advance on reflection. The distance curves corresponding to the position of maxima and minima are traced on a transparent overlay, the overlay being advanced one-half wavelength for successive maxima and minima. The intersection of successive distance lines gives the required height and phase change values. Figures 16-18 are the resulting overlays for the daytime data of 6 and 7 August. Figure 16 is for a free-space ground-wave velocity and figures 17 and 18 are for a ground-wave velocity of 0.14 per cent less than free space.

If the assumptions that this analysis is based upon are completely adequate, all distance curves would have a common intersection giving the proper value of height and phase change. In general, the points of intersection of adjacent distance lines are dispersed. Since the distance lines are nearly of the same slope, especially for 40 kc, relatively small errors in the location of maxima and minima would produce some spread in the points of intersection. From the theoretical work on vlf reflection coefficients by Wait and Perry[9] and by Budden[7], it appears that the assumptions this analysis is based upon are reasonable if the gradient of ionization at the lower edge of the ionosphere is high.

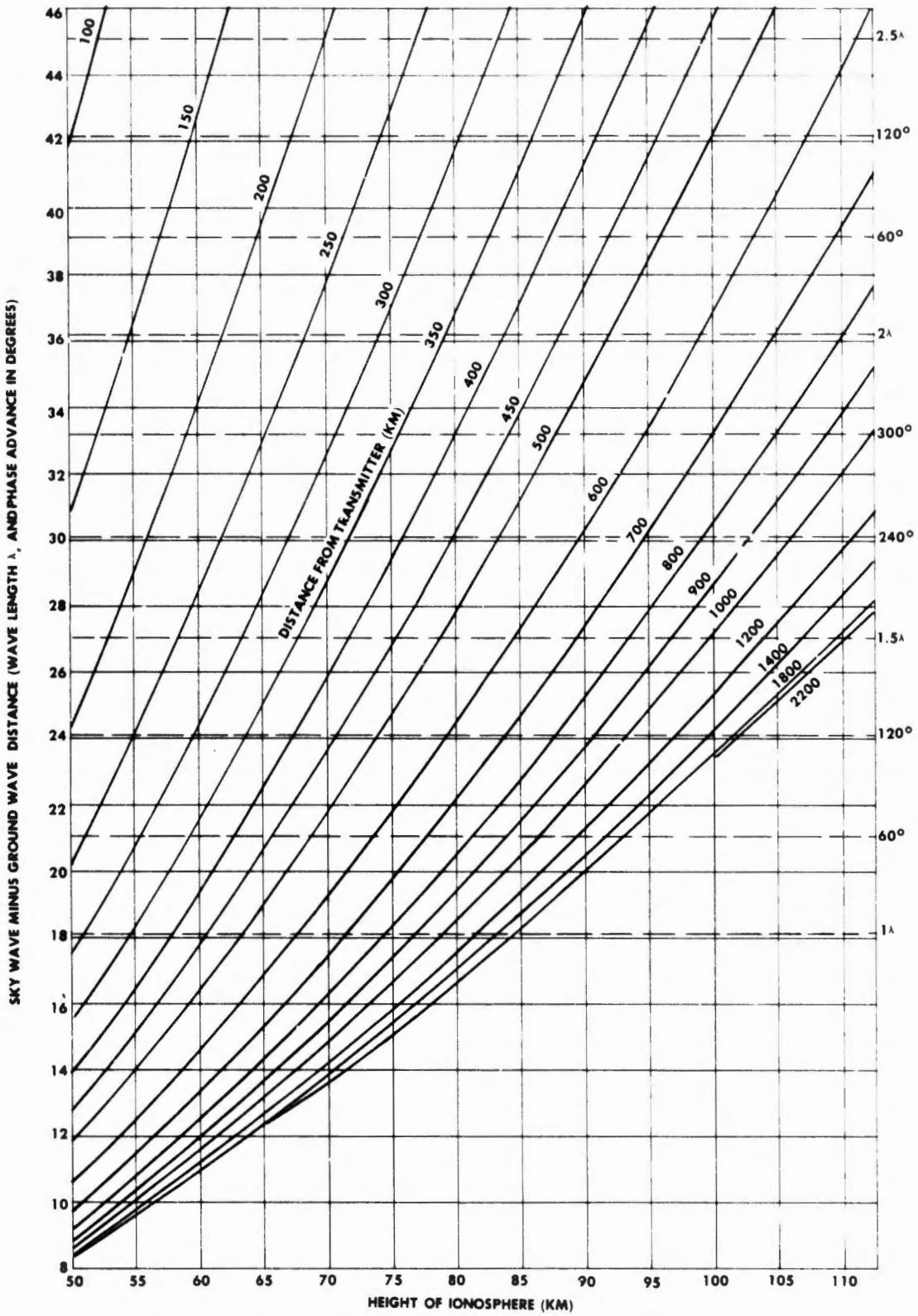

Figure 15. Geometrical relation between h', path length difference between ground wave and one-hop sky wave, and distance from transmitter.

Figure 16. Resulting overlays from analysis based on the assumption of equal height of reflection and equal phase change on reflection, between successive maxima and minima.

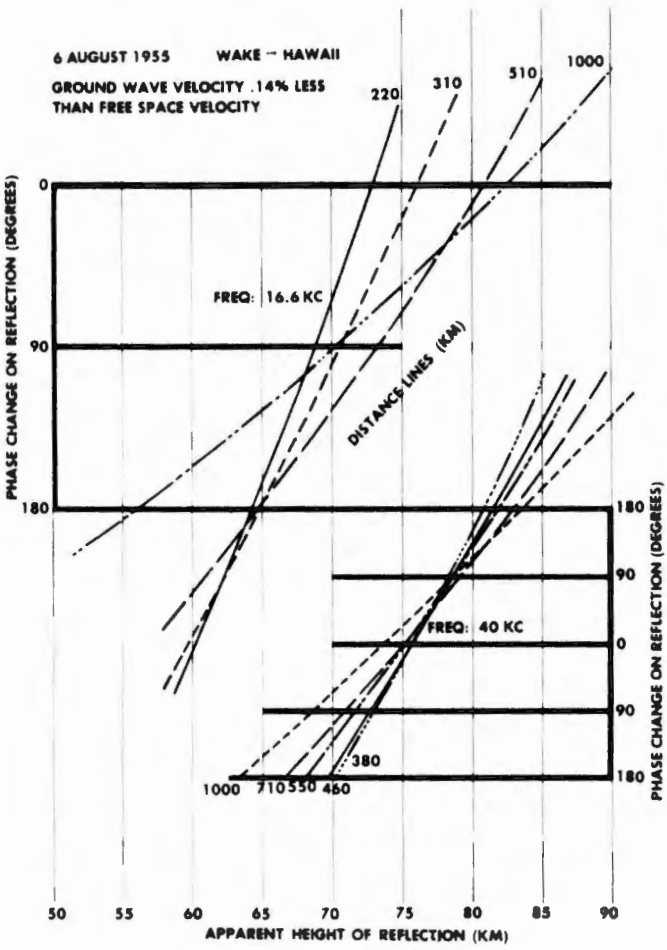

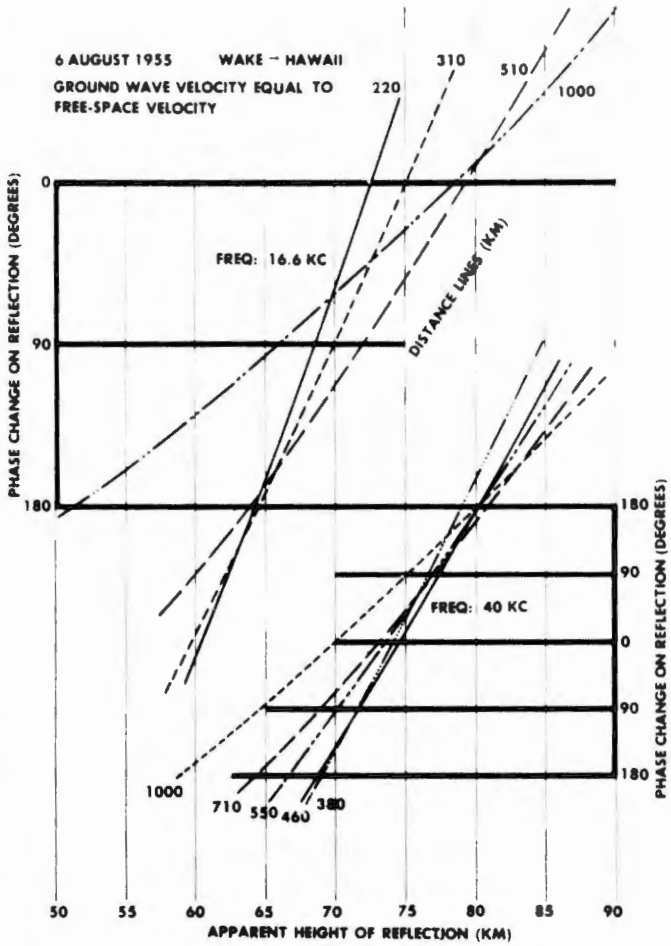

Figure 17. Resulting overlays from analysis based on the assumption of equal height of reflection and equal phase change on reflection, between successive maxima and minima.

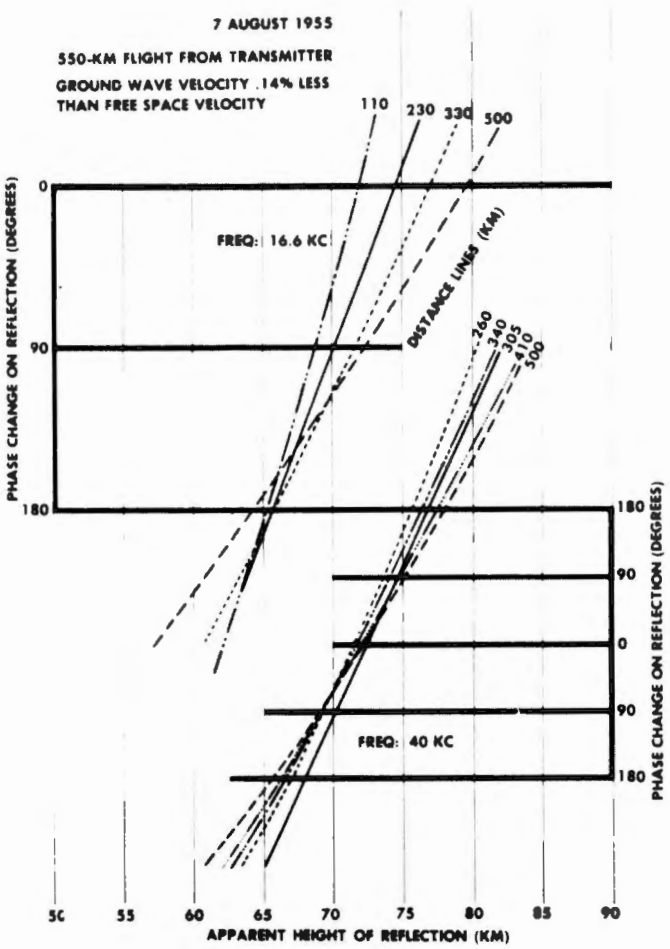

Figure 18. Resulting overlays from analysis based on the assumption of equal height of reflection and equal phase change on reflection, between successive maxima and minima.

Figures 19-26 show the reflection coefficient values determined from the data, as a function of angle of incidence measured from the normal to the reflecting layer. The angle of incidence was obtained assuming a 70-km reflecting height. The upper and lower limits represents the estimated experimental error. It appears that a quasi-Brewster angle effect exists for all reflection-coefficient curves with the possible exception of the results from the 6 August data shown in figure 24. The nearly identical reflection-coefficient curves of figures 21 and 23 are from data obtained on successive days, at the same time of day, and in the same direction from the transmitter. The other reflection coefficient curves were all obtained from data taken at various times of the day. The 16.6-kc and 40-kc coefficients are both less on 6 August than they were on the following day. Also, 40-kc reflection coefficients are less than the 16.6-kc coefficients when both were measured simultaneously.

Assuming the height of reflection and reflection coefficient values from the data of 6 August for distances within 1000 km of the transmitter, the field intensity from 800 to 6000 km was calculated, using the ray model concepts discussed in the preceding section. The amplitude and phase relation of the various sky-wave hops as a function of distance was determined and the resultant vector sum of the various modes was then computed. The phase relation was established by assuming a constant reflecting height of 77 km with no phase change on reflection. This is the height of reflection value at 930 km for the 6 August data of figure 11. The amplitudes of the various modes of propagation used are shown in figure 11. The amplitude of the n-hop sky wave out to $n \times 10^3$ kilometers was obtained by multiplying the unabsorbed n-hop intensity by $|R|^n$. From $n \times 10^3$ kilometers out to the limiting distance for the n-hop sky wave, the amplitude was determined by inspection with several different sets of amplitude curves assumed. From the limiting distance on, the amplitude was established by assuming the sky wave traveled as a ground wave around the curvature of the earth. The vector sums for each set of amplitude curves were obtained. The crosses indicate the resultants of the vector summation which most closely agree with the data.

Very good agreement between the data and the calculated amplitude exists out to 4000 km. Beyond 4000 km the calculations give results which

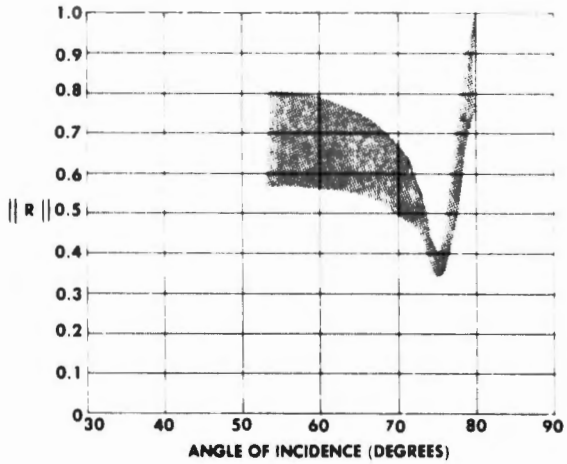

Figure 19. Daytime reflection coefficients, 16.6 kc, 8 December 1954.

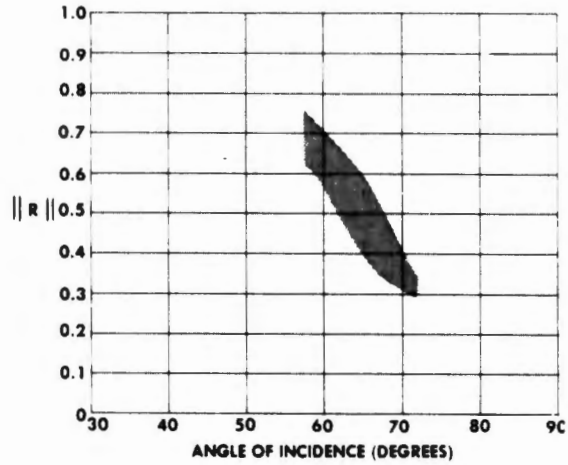

Figure 20. Daytime reflection coefficients, 16.6 kc, 7 August 1955.

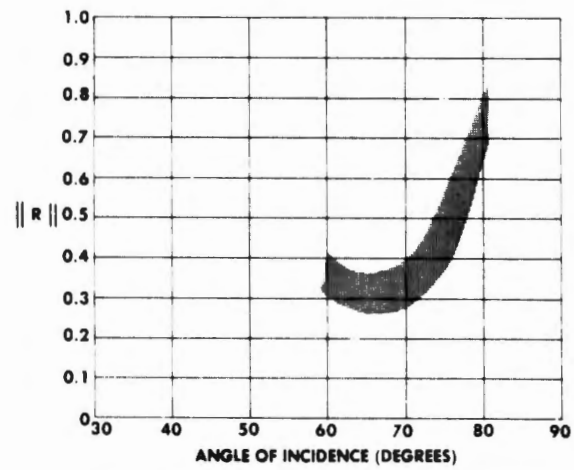

Figure 21. Daytime reflection coefficients, 16.6 kc, 10 August 1955 (a. m.).

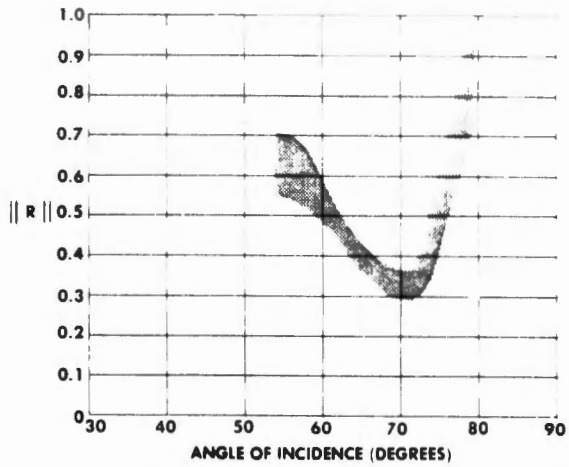

Figure 22. Daytime reflection coefficients, 16.6 kc, 10 August 1955 (p. m.).

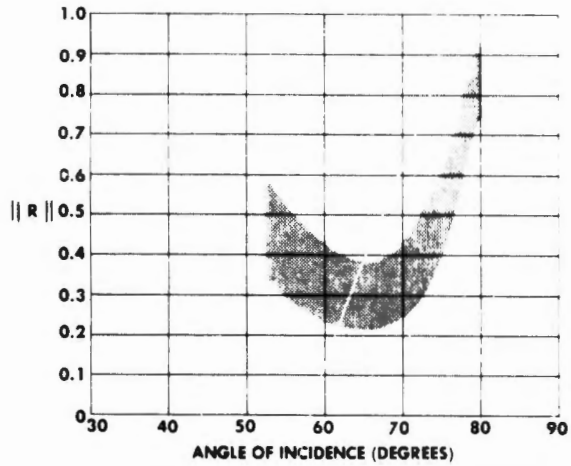

Figure 23. Daytime reflection coefficients, 16.6 kc, 11 August 1955.

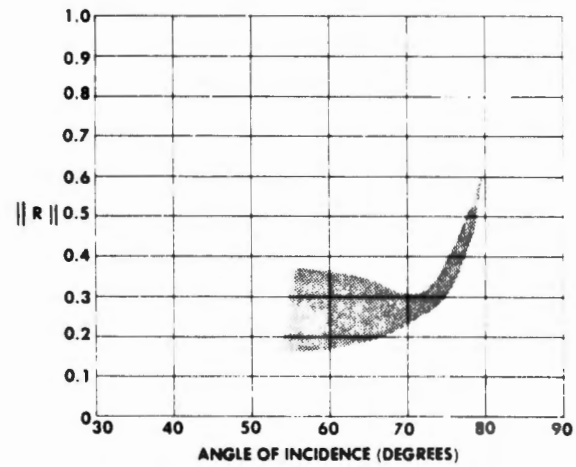

Figure 24. Daytime reflection coefficients, 16.6 kc, 6 August 1955.

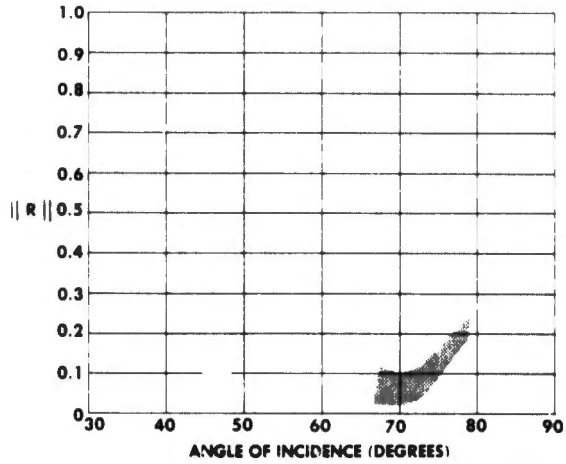

Figure 25. Daytime reflection coefficients, 40 kc, 6 August 1955.

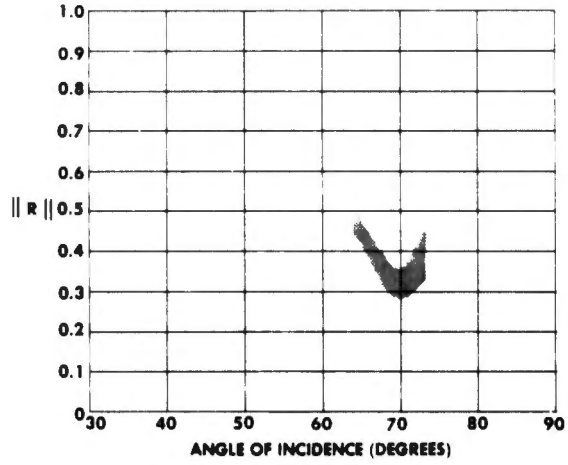

Figure 26. Daytime reflection coefficients, 40 kc, 7 August 1955.

are too low. This may be because the data beyond 4000 km were obtained on the previous day when different ionospheric conditions could have existed. The agreement of the calculated results with the data indicates that the ray theory concepts used in this report are useful for explaining the field intensities observed at large distances.

Results of Ray Theory Analysis of Nighttime Data

The data of figures 27-31 were recorded simultaneously during the nighttime flight from Hawaii to San Diego on 8-9 December 1954. The 16.6-kc, 19.8-kc, and 40-kc transmissions were from Hawaii and the 30-kc transmission was from San Diego. The height of reflection curves shown in each of the figures was determined by the method discussed in the section entitled "Ray Model Concepts Used in the Analysis of the Data." It is assumed for the analysis of this nighttime data that no phase change occurs on reflection from the ionosphere and that the ground-wave velocity is equal to the velocity of propagation in free space.

In order to determine which modes of propagation combine to produce the major maxima and minima, it was necessary to estimate the amplitude of the various sky waves. These estimated sky-wave amplitudes are shown in the figures. The continuation of the sky wave beyond the limiting distance as a ground wave was not considered for the nighttime data. The phase curves in the lower part of figures 27-31 indicating the in-phase and out-of-phase relationships between two modes of propagation are labeled according to the modes for which they are calculated.

Beyond the region where the ground wave and one-hop sky wave are dominant modes, it is difficult to determine which modes of propagation are responsible for the various maxima and minima. The major difficulty is that of finding a set of amplitudes and phase relationships of the various modes as a function of distance which is consistent for the several frequencies. It is difficult to find even a self-consistent variation of phase and amplitude as a function of distance for a single frequency, especially for the 40-kc data of figure 30. Part of the difficulty is due to the time variation of ionospheric conditions throughout the night. The simple assumptions upon which this ray theory analysis was based appear to be insufficient to explain the apparent inconsistencies. The amplitude curves for the various modes and the height of reflection curves are a preliminary representation and are not intended to represent completely the vector relations of the contributing modes.

Comparison of the height curves for the various frequencies indicates a general tendency for the height to increase to a maximum near the middle of the flight and decrease near the end. This may be due to a diurnal variation in height of reflection, or may result from the form of model used and the assumptions involved.

The amplitude and phase information of the individual propagation modes deduced from the 16.6-kc data of figure 27 were used to calculate the resultant vector amplitude as a function of distance. This calculated curve is shown in figure 31 together with the measured data for comparison. The height curve used for the calculation and shown in figure 31 differs from the height curve shown in figure 27 between 3000 and 4000 km. The curve of figure 31 represents the results obtained when an attempt was being made to keep the nighttime reflection-height variations to a minimum. The similarity between the measured and the calculated results again indicates that ray theory analysis is useful for explaining the variation with distance of vlf field intensities.

Figures 32 and 33 show the most recent nighttime data obtained. No analysis into components of the distant field intensities has been performed using this data. It is introduced primarily for the purpose of illustrating the variation in nighttime vlf field intensities as compared to the daytime field intensities recorded. Comparison of the 16.6-kc data of figure 32 with those of figure 27 shows a great similarity in signal amplitude as a function of distance. This illustrates that perhaps there is not very much difference between winter and summer nighttime vlf propagation conditions. However, there is quite a bit of difference between the data of figure 33 recorded during the night of 27 July 1955 and the data of figure 32 recorded during the previous night. These data were recorded in opposite directions from the same transmitter and may represent a difference in east-to-west and west-to-east propagation conditions. Unfortunately, the amount of data is insufficient to decide between this possibility and that of erratic night-to-night propagation conditions.

The reflection-coefficient values determined from the nighttime data are shown in figures 34-39. These values were determined in the same way they were

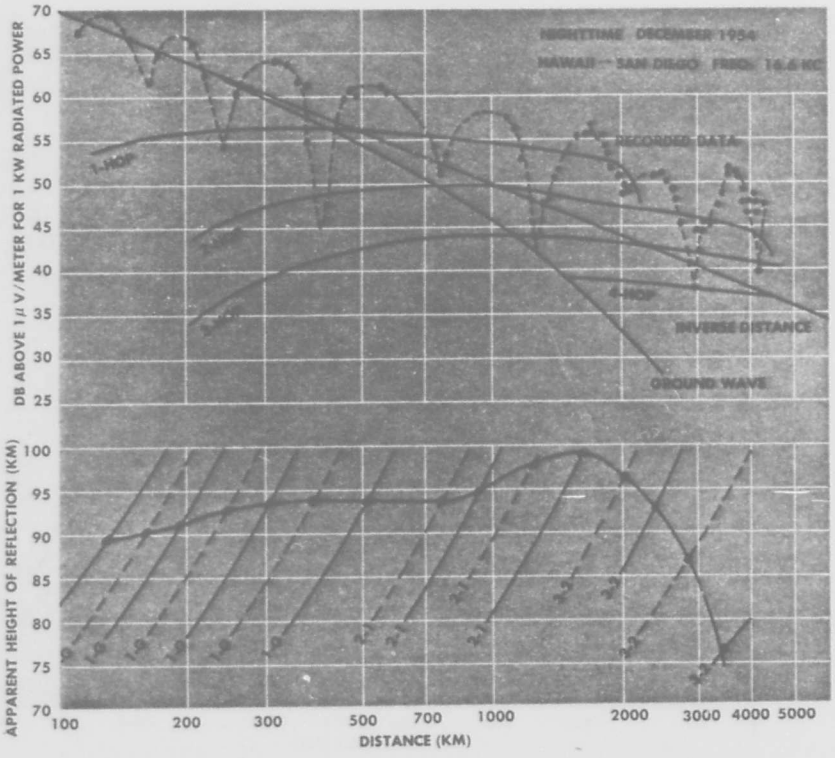

Figure 27. Plot of recorded data, estimated sky wave amplitudes, and height of reflection.

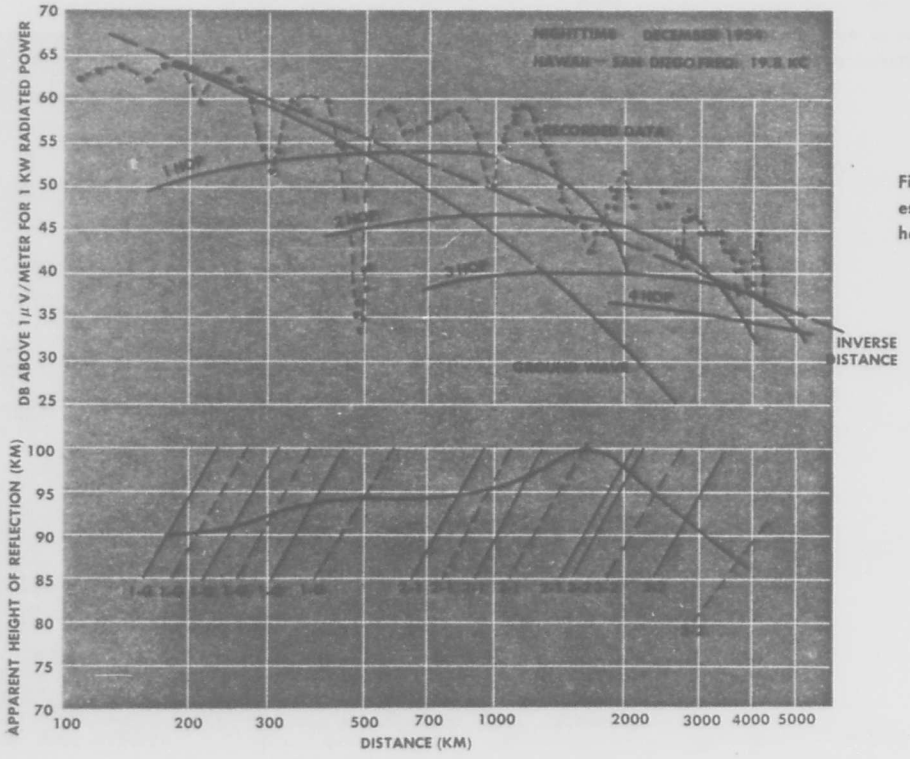

Figure 28. Plot of recorded data, estimated sky wave amplitudes, and height of reflection.

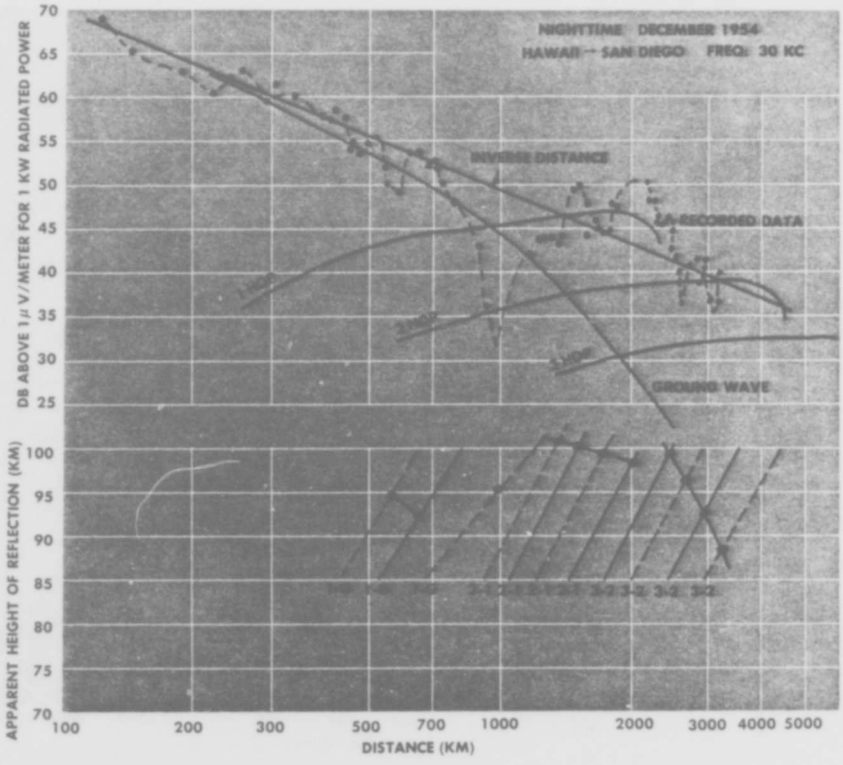

Figure 29. Plot of recorded data, estimated sky wave amplitudes, and height of reflection.

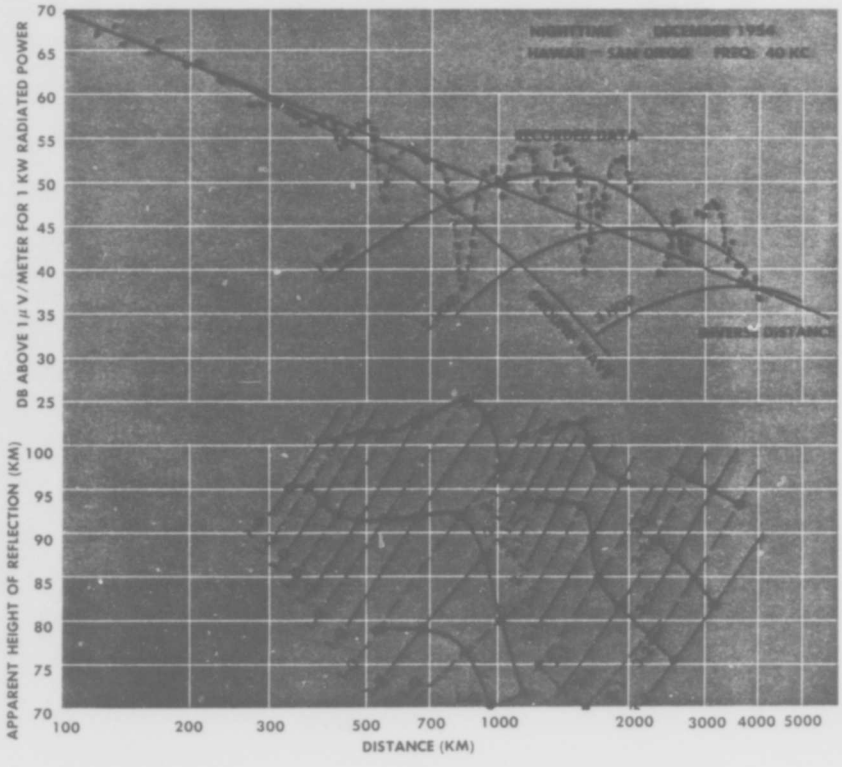

Figure 30. Plot of recorded data, estimated sky wave amplitudes, and height of reflection.

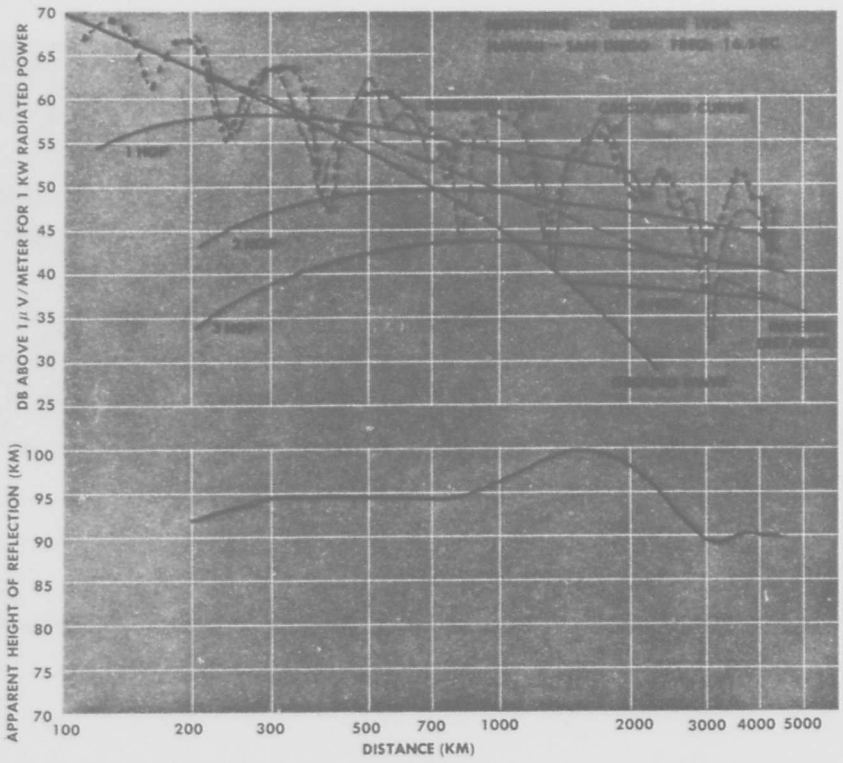

Figure 31. Comparison of recorded data with calculations based on ray theory.

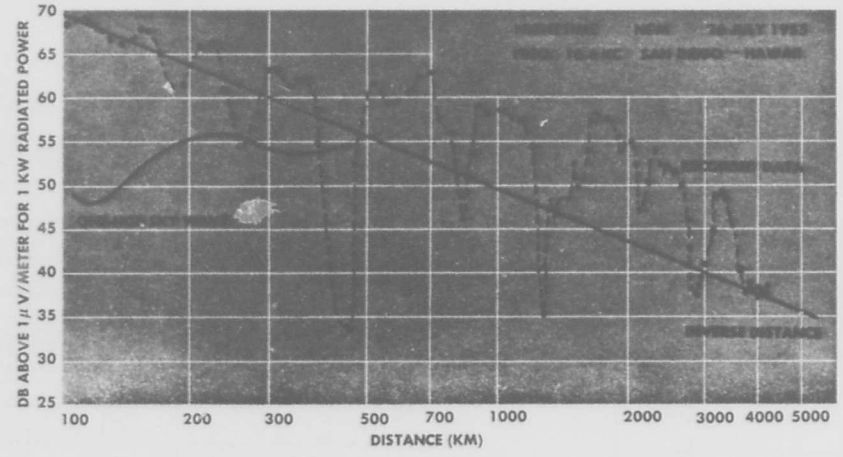

Figure 32. Plot of recorded data and one-hop sky-wave amplitude.

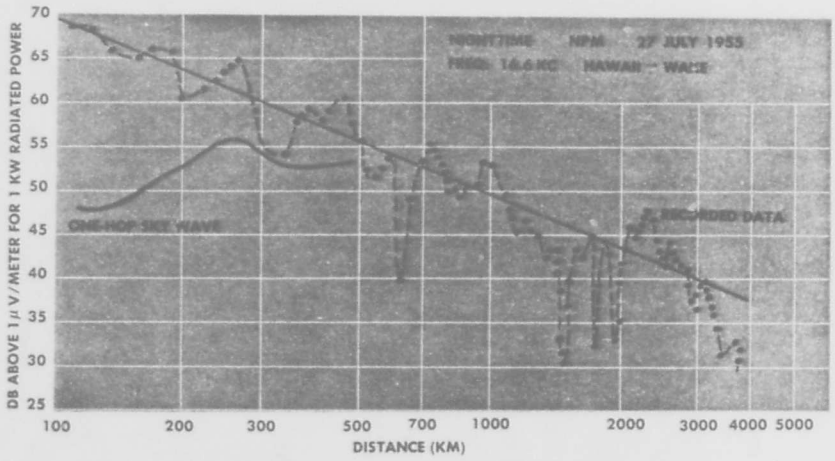

Figure 33. Plot of recorded data and one-hop sky-wave amplitude.

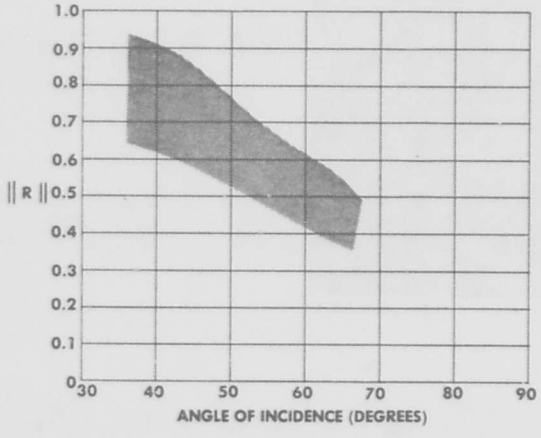

Figure 34. Nighttime reflection coefficients, 16.6 kc, 8 December 1954.

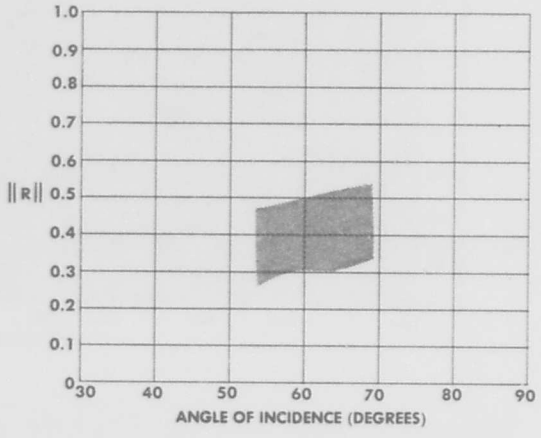

Figure 35. Nighttime reflection coefficients, 19.8 kc, 8 December 1954.

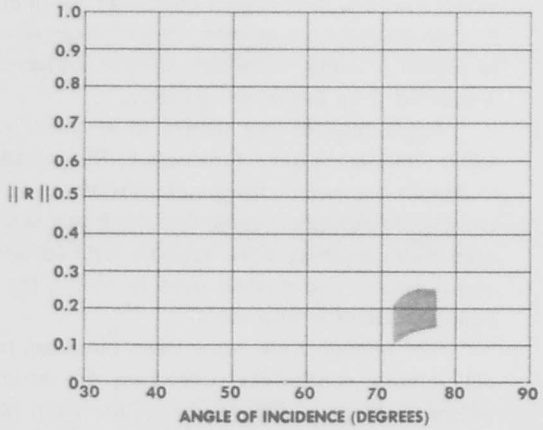

Figure 36. Nighttime reflection coefficients, 30 kc, 8 December 1954.

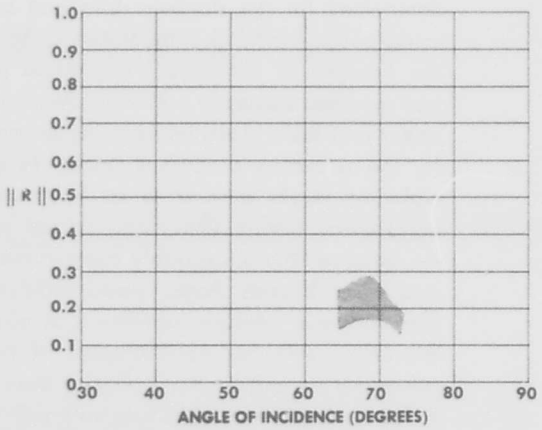

Figure 37. Nighttime reflection coefficients, 40 kc, 8 December 1954.

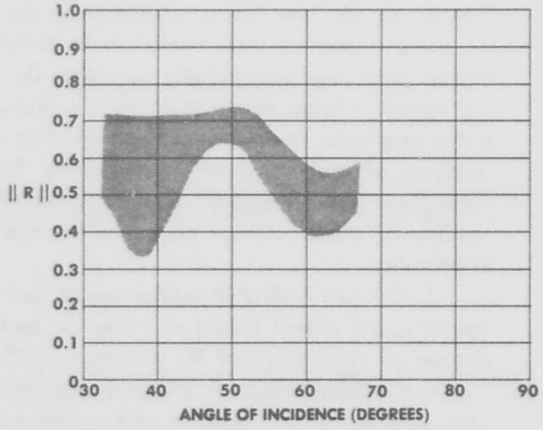

Figure 38. Nighttime reflection coefficients, 16.6 kc, 26 July 1955.

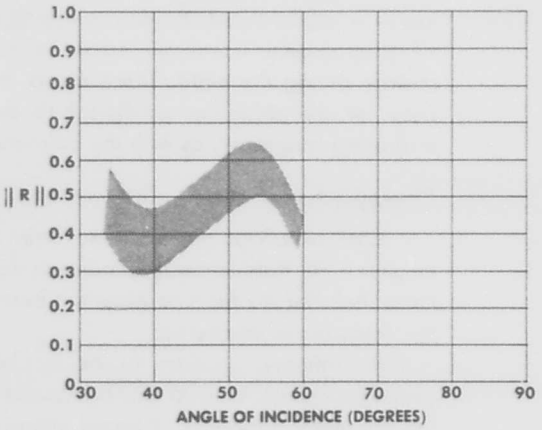

Figure 39. Nighttime reflection coefficients, 16.6 kc, 27 July 1955.

determined for the daytime data and as explained in the section entitled "Ray Model Concepts Used in the Analysis of the Data." The angle of incidence was obtained assuming a 90-km reflecting height. The upper and lower limits indicate the estimated bounds for the reflection coefficient values. In general, the nighttime results appear to be less consistent than the daytime results. They are also less reliable than the daytime results, probably more so than the upper and lower bounds shown would indicate. The two-hop sky wave becomes significant at about 500 km, interfering with the determination of the reflection coefficient at angles more oblique than about 70°. At shorter distances, there are an insufficient number of measured points to determine accurately the position of maxima and minima or their amplitudes. The best 16.6-kc data are those for 26 and 27 July but the reflection-coefficient curves for those dates are the most irregular. It is reasonable to expect irregularity in nighttime reflection-coefficient results since vlf propagation conditions seem to change more rapidly during the night. There seems to be a tendency for the reflection coefficient to decrease with increasing frequency, as with the daytime results.

Conclusions

Comparison of the airplane data with various empirical vlf field-intensity prediction formulas indicates that Pierce's formula gives the best estimate for the frequencies measured.

Ray theory appears to be applicable to vlf propagation out to 6000 km. It is useful for explaining the major variations of signal intensity as a function of distance for both daytime and nighttime conditions. However, at large distances the ray model becomes increasingly difficult to use in practice. It is necessary to make many simplifying assumptions to obtain a model for which the parameters can be evaluated from the measured data.

Application of ray theory to vlf measurements within 1000 km is quite satisfactory. The method used to obtain the actual height of reflection and phase change on reflection from the simultaneously measured multifrequency data appears justified and gives useful results. The method used to obtain the reflection coefficients is also useful.

Not enough data have been obtained to draw any definite conclusions concerning the variation of vlf field intensities with season of the year, direction of propagation, attenuation over land vs over water, or latitude effects.

Recommendations

1. Make additional recordings of vlf signal intensities by airplane, under the following conditions: (a) using improved instrumentation to obtain continuous recordings and greater accuracy; (b) recording signal to large distances to obtain propagation paths over land; and (c) continuing simultaneous recordings of multifrequency transmissions from the same general location to obtain ionospheric reflection coefficients, phase change on reflection, and height of reflection.

2. Conduct further investigations of methods for obtaining (a) actual height of reflection and phase change on reflection and (b) reflection coefficients.

3. Continue study of effects of season of the year, direction of propagation, attenuation over land vs attenuation over water, and latitude effects on variation of vlf field intensities.

References

1. K. Weekes "The Ground Interference Pattern of Very-Low-Frequency Radio Waves" *Institution of Electrical Engineers. Proceedings* vol. 97, part 3, no. 46, March 1950, pp. 100-107.

2. K. G. Budden "The Propagation of Very-Low-Frequency Radio Waves to Great Distances" *Philosophical Magazine* vol. 44, no. 352, May 1953, pp. 504-513.

3. F. A. Kitchen *et al.* "A Review of Present Knowledge of the Ionospheric Propagation of Very-Low-, Low-, and Medium-Frequency Waves" *Institution of Electrical Engineers. Proceedings* vol. 100, part 3, no. 64, March 1953, pp. 100-108.

4. J. A. Pierce *Sky-Wave Field Intensity I: Low- and Very-Low Radio Frequencies* (Harvard University. Cruft Laboratory, Technical Report 158) 1 September 1952.

5. K. A. Norton "The Calculation of Ground-Wave Field Intensity over a Finitely Conducting Spherical Earth" *Institute of Radio Engineers. Proceedings* vol. 29, no. 12, December 1941, pp. 623-639.

6. F. E. Terman *Radio Engineers' Handbook* McGraw-Hill, 1943, pp. 700-707.

7. K. G. Budden "The Numerical Solution of the Differential Equations Governing the Reflection of Long Radio Waves from the Ionosphere II" *Royal Society of London. Philosophical Transactions* series A, vol. 248, no. A-939, 12 May 1955, pp. 45-72.

8. E. B. Mendoza "A Method of Determining the Velocity of Radio Waves over Land on Frequencies near 100 kc" *Institution of Electrical Engineers. Proceedings* vol. 94, part 3, no. 32, November 1947, pp. 396-398.

9. J. R. Wait and L. B. Perry *Calculations of Ionospheric Reflection Coefficients at Very-Low Radio Frequencies* (National Bureau of Standards, Report 3588) 15 May 1956.

Navy Electronics Laboratory
Report 767

AN EXPERIMENTAL MEASUREMENT OF VLF FIELD-STRENGTH AS A FUNCTION OF DISTANCE USING AN AIRCRAFT, by J. E. Bickel, J. L. Heritage, and S. Weisbrod. 27 p., 28 January 1957. UNCLASSIFIED

The variation of vlf field intensities with distance was recorded in an airplane to distances of 7600 km. It is found to be in closer agreement with Pierce's vlf prediction formula than any other existing formula. The observed interference pattern is satisfactorily explained on the basis of a ray model of propagation. Several graphical methods of analysis have been applied to the data and values have been obtained for reflection coefficient and phase change on reflection at the ionosphere and for the height of reflection of vlf sky waves.

1. Field strength — Measurement

I. Bickel, J. E.

II. Heritage, J. L.

III. Weisbrod, S.

SR 06401
NE 120000-839.7 (NEL M2-1)

This card is UNCLASSIFIED

Navy Electronics Laboratory
Report 767

AN EXPERIMENTAL MEASUREMENT OF VLF FIELD-STRENGTH AS A FUNCTION OF DISTANCE USING AN AIRCRAFT, by J. E. Bickel, J. L. Heritage, and S. Weisbrod. 27 p., 28 January 1957. UNCLASSIFIED

The variation of vlf field intensities with distance was recorded in an airplane to distances of 7600 km. It is found to be in closer agreement with Pierce's vlf prediction formula than any other existing formula. The observed interference pattern is satisfactorily explained on the basis of a ray model of propagation. Several graphical methods of analysis have been applied to the data and values have been obtained for reflection coefficient and phase change on reflection at the ionosphere and for the height of reflection of vlf sky waves.

1. Field strength — Measurement

I. Bickel, J. E.

II. Heritage, J. L.

III. Weisbrod, S.

SR 06401
NE 120000-839.7 (NEL M2-1)

This card is UNCLASSIFIED

Navy Electronics Laboratory
Report 767

AN EXPERIMENTAL MEASUREMENT OF VLF FIELD-STRENGTH AS A FUNCTION OF DISTANCE USING AN AIRCRAFT, by J. E. Bickel, J. L. Heritage, and S. Weisbrod. 27 p., 28 January 1957. UNCLASSIFIED

The variation of vlf field intensities with distance was recorded in an airplane to distances of 7600 km. It is found to be in closer agreement with Pierce's vlf prediction formula than any other existing formula. The observed interference pattern is satisfactorily explained on the basis of a ray model of propagation. Several graphical methods of analysis have been applied to the data and values have been obtained for reflection coefficient and phase change on reflection at the ionosphere and for the height of reflection of vlf sky waves.

1. Field strength — Measurement

I. Bickel, J. E.

II. Heritage, J. L.

III. Weisbrod, S.

SR 06401
NE 120000-839.7 (NEL M2-1)

This card is UNCLASSIFIED

Navy Electronics Laboratory
Report 767

AN EXPERIMENTAL MEASUREMENT OF VLF FIELD-STRENGTH AS A FUNCTION OF DISTANCE USING AN AIRCRAFT, by J. E. Bickel, J. L. Heritage, and S. Weisbrod. 27 p., 28 January 1957. UNCLASSIFIED

The variation of vlf field intensities with distance was recorded in an airplane to distances of 7600 km. It is found to be in closer agreement with Pierce's vlf prediction formula than any other existing formula. The observed interference pattern is satisfactorily explained on the basis of a ray model of propagation. Several graphical methods of analysis have been applied to the data and values have been obtained for reflection coefficient and phase change on reflection at the ionosphere and for the height of reflection of vlf sky waves.

1. Field strength — Measurement

I. Bickel, J. E.

II. Heritage, J. L.

III. Weisbrod, S.

SR 06401
NE 120000-839.7 (NEL M2-1)

This card is UNCLASSIFIED

INITIAL DISTRIBUTION LIST

(One copy to each addressee unless otherwise specified)

Chief, Bureau of Ships (Code 312) (12 copies)
Chief, Bureau of Ordnance (Re6) (Add) (2)
Chief, Bureau of Aeronautics (TD-414)
Chief of Naval Operations (Op-37) (2)
Commander in Chief, U. S. Pacific Fleet
Commander in Chief, U. S. Atlantic Fleet
Commander Operational Development Force, U. S. Atlantic Fleet
Commander, U. S. Naval Air Development Center (Library)
Commander, U. S. Naval Air Missile Test Center (Technical Library)
Commander, U. S. Naval Air Test Center (NANEP) (2)
Commander, U. S. Naval Ordnance Laboratory (Library) (2)
Commander, U. S. Naval Ordnance Test Station (Pasadena Annex Library)
Commander, U. S. Naval Proving Ground
Commanding Officer and Director, David Taylor Model Basin (Library) (2)
Commanding Officer and Director, U. S. Navy Underwater Sound Laboratory (Code 1450) (3)
Director, U. S. Naval Engineering Experiment Station (Library)
Director, U. S. Naval Research Laboratory (Code 2021) (2)
Director, U. S. Navy Underwater Sound Reference Laboratory (Library)
Commanding Officer, Office of Naval Research, Pasadena Branch
Senior Navy Liaison Officer, U. S. Navy Electronics Liaison Office
Superintendent, U. S. Naval Postgraduate School (Library) (2)
Assistant Secretary of Defense (Research and Development) (Technical Library Branch)
Assistant Chief of Staff, G-2, U. S. Army (Document Library Branch) (3)
Chief of Engineers, U. S. Army (Engineer Research and Development Division, Field Engineering Branch)
The Chief of Psychological Warfare, U. S. Army
Chief Signal Officer, U. S. Army (Engineering and Technical Division, Engineering Control Branch, SIGGD)
Commanding General, Aberdeen Proving Ground (Technical Information Branch)
Commanding General, Army Electronic Proving Ground (Department of Electronic Warfare) (Engineering and Technical Department)
Commanding General, The Artillery Center
Commanding General, Redstone Arsenal (Technical Library)
Commanding General, Signal Corps Engineering Laboratories (Administrative Division, Technical Documents Center)
Commanding Officer, Army Chemical Center (Technical Library)
Commanding Officer, Engineer Research and Development Laboratories (Technical Documents Center)
Commanding Officer, Office of Ordnance Research
Commanding Officer, White Sands Signal Corps Agency (SIGWS-AD-2)
Chief, Army Field Forces (ATDEV-8)
President, Army Field Forces Board No. 1

Deputy Chief of Staff, Development, U. S. Air Force (AFDRD-RE)
(AFDRD-CC)
Deputy Chief of Staff, Operations, U S. Air Force (AFOAC-P F)
Commander, Air Defense Command
(Director of Communications and Electronics, AC&W Coordinating Division)
(Office of Operations Analysis, John J. Crowley)
Commander, Air Research and Development Command (RDDPA)
Commander, Air University (Air University Library, CR-5028)
Commander, Alaskan Air Command
(Director of Communications and Electronics)
(Chief, Operations Analysis Office)
Commander, Strategic Air Command
(Operations Analysis)
Commander, Air Force Armament Center (ACGL)
Commander, Air Force Cambridge Research Center (CRQSL-1)
Commander, Air Force Missile Test Center
(Classified Information Section)
Commander, Air Force Special Weapons Center
(Air Force Atomic Energy Library)
Commander, Rome Air Development Center (RCRES-4C)
Commander, Wright Air Development Center (Technical Information Control Office, WCOSI)
Commander, Holloman Air Force Base (HDOTE-1)
Chief, Los Angeles Air Force Development Field Office
Director, Langley Aeronautical Laboratory
Chief, U. S. Weather Bureau
Director, National Bureau of Standards (Central Radio Propagation Laboratory Library)
Chief, Central Radio Propagation Laboratory (K. A. Norton), Boulder, Colorado
Chairman, Federal Communications Commission (Chief Engineer)
Director of Development, Air Navigation Development Board, Civil Aeronautics Administration (W-9)
Brown University, Chairman of the Department of Physics
University of California, Director, Antenna Laboratory (Professor T. C. McFarland)
University of California at Los Angeles, Engineering Department (Dr. F. W. Schatt)
California Institute of Technology, Chief, Reports Group (I. E. Newlan), Jet Propulsion Laboratory
Colorado College, Department of Physics (Dr. P. E. Boucher)
Cornell University, School of Electrical Engineering (Dr. Charles R. Burrows) (Dr. Henry G. Booker)
Dartmouth College, Thayer School of Engineering (Millett G. Morgan)
Georgia Institute of Technology, Head, Physics Division, State Engineering Experiment Station (J. E. Boyd)
Harvard Observatory (D. H. Menzel)
The Johns Hopkins University, Department of Physics (D. E. Kerr, Assistant Professor)
The Johns Hopkins University, Applied Physics Laboratory (Dr. F. N. Frenkiel), Silver Spring, Md.
Massachusetts Institute of Technology
Director, Research Laboratory of Electronics
Weather Radar Project
Massachusetts Institute of Technology, Lincoln Laboratory (Dr. T. J. Carroll), Lexington, Mass.
University of Michigan, Electrical Engineering Department (Professor S. S. Attwood)
New York University, Project Director, Washington Square College, Mathematics Research Group (Morris Kline)
Stanford University, Electronics Research Laboratory (Dr. Alan T. Waterman, Jr.)
The University of Texas
Director, Electrical Engineering Research Laboratory
Yale University
Sloane Physics Laboratory (Prof. H. Margenau)
Bell Telephone Laboratories, Incorporated, Murray Hill, New Jersey
(S. A. Schelkunoff)
Bell Telephone Laboratories, Incorporated
(Holmdel Laboratory Library)
Collins Radio Company, Research and Development Division (I. H. Gerks)
Federal Telecommunication Laboratories, Incorporated (Technical Library)
Sperry Gyroscope Company (Engineering Library)
Vitro Corporation of America, Silver Spring Laboratory (Library)

VIA BUREAU OF SHIPS:

The Admiral, British Joint Services Mission (Navy Staff) (3)

NAVY — NEL San Diego, Calif.